

# REVIEW OF NEW DEVELOPMENTS IN SUPERCONDUCTING UNDULATOR TECHNOLOGY AT THE APS\*

J.D. Fuerst†, Y. Ivanyushenkov, Q. Hasse, M. Kasa, I. Kesgin, Y. Shiroyanagi, E. Gluskin,  
 Argonne National Laboratory, Argonne, IL, USA

## Abstract

Superconducting undulator technology for storage ring light sources has evolved from proof of principle to the working insertion device level. Both planar and helical magnet topologies using NbTi superconductor have been successfully incorporated into functional devices operating in the Advanced Photon Source (APS) storage ring at liquid helium temperatures using cryocooler-based, zero-boil-off refrigeration systems. Development work on higher field magnets using Nb<sub>3</sub>Sn superconductor is ongoing at the APS, as are concepts for FEL-specific magnets and cryostats for future light sources.

## BACKGROUND – EXISTING DEVICES

The APS currently operates three SCUs in the storage ring. Two are nominally identical vertical gap planar devices with period length 1.8 cm and overall active length 1.1 m. These devices reside in Sectors 1 and 6. The third is a helically wound, circularly polarizing device located in Sector 7 with period length 3.15 cm and overall active length 1.2 m. Device parameters are listed in Table 1.

Table 1: Parameters for SCUs Installed at APS

Parameter	Value	
	Planar	Helical
Cryostat length [m]	2.06	1.85
Magnetic length [m]	1.1	1.2
Period [mm]	18	31.5
Magnetic gap [mm]	9.5	29 (diameter)
Beam chamber aperture [mm]	7.2	8(V) x 26(H)
Peak field [T]	0.97	0.42 (B <sub>x</sub> =B <sub>y</sub> )
K value	1.63	1.2 (K <sub>x</sub> =K <sub>y</sub> )

Additional details regarding the existing devices as well as a fourth planar device developed for LCLS R&D are provided in [1,2]. For details on magnetic performance see [3]. Table 2 lists the operational statistics for planar device SCU18-1 which has operated in Sector 1 of the APS storage ring since May 2015. Device performance has been highly reliable, with overall availability of 99.99%. Figures 1 and 2 show the devices installed in the APS storage ring.

\*Work supported by the U.S. Department of Energy, Office of Science under Contract No. DE-AC02-06CH11357

† fuerst@anl.gov

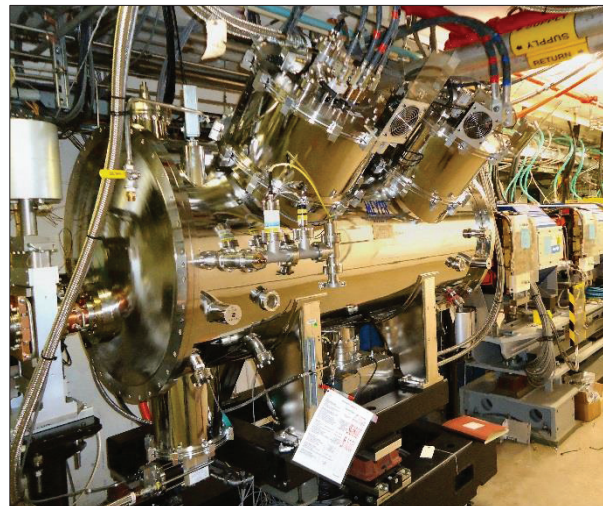


Figure 1: Planar SCU installed in the APS ring, Sector 1.



Figure 2: Helical SCU installed in Sector 7.

Table 2: Operating Statistics for SCU18-1

Year	SCU hours operating	Availability %
2015	3059	99.997
2016	4585	99.990
2017	4818	99.984

# THE LCLS-II-HE, A HIGH ENERGY UPGRADE OF THE LCLS-II\*

T.O. Raubenheimer<sup>†</sup>, for LCLS-II/LCLS-II-HE Collaborations  
 SLAC National Accelerator Laboratory, Menlo Park, USA

## Abstract

The LCLS-II is a CW X-ray FEL covering a photon spectral range from 200 to 5,000 eV. It is based on a 4 GeV SRF linac installed in the 1<sup>st</sup> km of the SLAC linac tunnel. This paper will describe a high energy upgrade, referred to as the LCLS-II-HE, which will increase the beam energy to 8 GeV and the photon spectral range to 12.8 keV; this range may be extended through 20 keV with improvements of the electron injector and beam transport. The LCLS-II-HE received the US DOE CD-0 approval, Mission Need, and has developed a CDR in support of a CD-1 review scheduled for summer 2018.

## INTRODUCTION

The development of X-ray free-electron lasers (XFELs) has launched a new era in X-ray science by providing ultrafast coherent X-ray pulses with a peak brightness that is nearly one billion times higher than previous X-ray sources. As the world's first hard X-ray FEL, the LCLS has already demonstrated tremendous scientific impact across broad areas of science, based on fundamental studies of the behavior of matter at the atomic length scale and femtosecond timescale. A comprehensive scientific overview of the first five years of LCLS operation was recently published [1]. Numerous similar facilities are just beginning operation or are under construction around the world [2].

While the LCLS has delivered unprecedented peak brightness, with a repetition rate of 120 Hz, the average brightness is modest, similar to that of a synchrotron source. Furthermore, many experiments require attenuation of the peak intensity in order to avoid perturbation of the sample by the X-ray probe. In these cases, signal accumulation times often become prohibitive, thus rendering many experiments impractical. The LCLS-II will provide ultrafast X-rays in the soft and tender X-ray range (0.2-5 keV) at repetition rates up to 1 MHz with two independent XFELs based on adjustable-gap undulators: a soft X-ray undulator (SXU) covering the range from 0.2 to 1.3 keV, and a hard X-ray undulator (HXU) covering the range from 1 to 5 keV. This development is driven by important new science opportunities that have been identified and advanced over the past decade through scientific workshops, both in the U.S. and around the world [3].

The extension of the LCLS-II to the hard X-ray regime is motivated by the scientific need for precision measurements of structural dynamics on atomic spatial scales and fundamental timescales. Such measurements are essential for addressing many of the transformative op-

portunities identified in the latest report from the Basic Energy Sciences Advisory Committee (BESAC) [4], and will provide detailed insight into the behavior of complex matter, real-world heterogeneous samples, functioning assemblies, and biological systems on fundamental scales of energy, time, and length. The LCLS-II High Energy Upgrade (LCLS-II-HE) is a natural extension to LCLS-II, extending the high-repetition-rate capabilities into the critically important “hard X-ray” regime (spanning from 5 keV to at least 12.8 keV and potentially up to 20 keV) that has been used in more than 75% of the LCLS experiments to date.

The LCLS-II-HE upgrade will build on the LCLS-II, described in Refs. [5] and [6], and will add significant capability to the facility. The changes in the LCLS-II capability are summarized below and illustrated in Fig. 1.

- The photon spectral range from the hard X-ray undulator at MHz-rate will be extended from 1 – 5 keV to 1 – 12.8 keV using electrons beams with energies between 3.3 and 8 GeV with the possibility of X-ray energies approaching 20 keV given the success of off-project R&D programs;
- The hard X-ray undulator will include the capability for self-seeding the MHz-rate X-ray beam;
- The soft X-ray undulator will be able to produce X-rays between 0.2 and 1.3 keV or access the tender X-ray region between 1 – 5 keV at MHz-rates coincidentally with the production of MHz-rate hard X-rays;
- The hard X-ray beamlines and instruments will be upgraded to maximize the science from the MHz-rate high energy FEL beams;
- And, the hard X-ray experimental hall will be modified to incorporate an additional experimental instrument and also better optimize the usage of the existing instruments;
- The performance of LCLS and LCLS-II operational modes and techniques will not be negatively impacted by the LCLS-II-HE including the generation of X-ray pulses with high peak power (100's of GW) at 120 Hz using the copper linac.

The layout of the LCLS-II-HE accelerator is shown schematically in Fig. 2. The facility will use the existing accelerator tunnels at SLAC. The increase in beam energy from LCLS-II to LCLS-II-HE is due to an increase in acceleration gradient and an increase in the SRF linac length. In particular, the SRF linac will be extended to fill the first km of the existing SLAC linac tunnel which has been largely cleared of legacy equipment.

To construct the LCLS-II-HE, SLAC will continue the partnership with other national laboratories having recent technical leadership in the critical SRF technologies. In a

\* Work supported by US DOE Contract No. DE-AC02-76SF00515.

<sup>†</sup> torr@stanford.edu

# LATTICE DESIGN FOR PETRA IV: TOWARDS A DIFFRACTION-LIMITED STORAGE RING

I. Agapov \*, R. Brinkmann, Y.-C. Chae, X.N. Gavalda, J. Keil, R. Wanzenberg,  
 Deutsches Elektronen Synchrotron, Notkestrasse 85, Hamburg, Germany

## Abstract

Machine design for the PETRA III storage ring upgrade – PETRA IV – aiming at a 10-30 pm emittance range has been ongoing at DESY. We present the design challenges and approaches for this machine, the baseline lattice and the alternative lattice concepts currently under consideration.

## INTRODUCTION

PETRA III has been in operation as a synchrotron radiation user facility since 2009 [1, 2], being at the time of construction the world's record holder for the smallest electron beam emittance (1 nm rad at 6 GeV) among hard x-ray sources. An extension project has been ongoing since 2014 [3], and potential of reducing the emittance with the existing lattice comprising a mixture of DBA and FODO cells has been studied [4], putting the ultimate emittance of such lattice type at around 500 pm for PETRA circumference of 2304 meters. With the advance of the multi-bend achromat (MBA) technology pioneered by MAX IV, many light sources, and among them all large hard x-ray facilities – ESRF, APS, and SPRING 8 – have proposed machine upgrades reducing the emittance by orders of magnitude. With PETRA IV design studies [5] DESY has started the preparation phase for the MBA-based upgrade project which will be essential to maintain the laboratory's role in cutting edge research with synchrotron radiation.

## DESIGN OBJECTIVES

The upgrade plan of PETRA III to PETRA IV aims at building a unique light source, with an ultra-low horizontal emittance in the range between 10 pm rad and 30 pm rad at a beam energy of 6 GeV. In addition to the three existing experimental halls in the northeast of the storage ring, it is foreseen to build a new experimental hall in the southwest just opposite to the Max von Laue Hall. The general layout of PETRA IV is shown in Fig. 1. The storage ring will provide 18 straight sections of approximately 5 m length and four longer straight sections in the four experimental halls. With canting four straight sections and splitting another four undulator beams by appropriate optics, thirty parallel undulator stations could be realised. The first beamline in each experimental hall has its undulator located in the long straight sections separating the arcs. For these four beamlines, the undulator length is not limited by length of the straight section but only by the available acceptance and the electron beam parameters (e. g.,  $\beta$ -functions) can be optimised for highest possible brightness. Fig. 2 shows the brightness that

could be reached with PETRA IV in one of the four long straight sections. Ultra-low emittance and a reduced number of electron bunches for timing experiments are conflicting design goals that can not be met with a single mode of operation of PETRA IV. Therefore, it is planned to provide two operation modes for PETRA IV, the high-brightness, high-coherence continuous mode and a timing mode with fewer bunches with increased bunch charge but with larger emittance and thus slightly reduced brightness.



Figure 1: Layout of the PETRA IV facility.

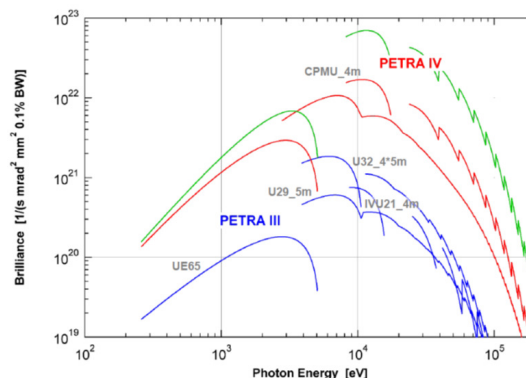


Figure 2: Comparison of brightness between PETRA III and PETRA IV. Red curve:  $\epsilon_x = 15$  pm,  $\kappa = 100\%$ ,  $\beta_x = 5$  m,  $\beta_y = 2.5$  m. Green curve:  $\epsilon_x = 10$  pm,  $\kappa = 50\%$ ,  $\beta_x = 1$  m,  $\beta_y = 1$  m.

For lattices in the 10-30 pm range the intra-beam scattering plays an important role and limits the emittance that can be achieved in practice with reasonable bunch charges (see e.g. Figure 3). Although the zero-current emittance scales with beam energy as  $\gamma^{-2}$ , IBS changes this dependency as shown in Figure 4 (calculations for the reference lattice), and the beam energy of approx. 6 GeV appears optimal for emittance minimization.

The insertion devices have significant impact on beam parameters, providing emittance damping or emittance blow-up depending on ID field strength, ID length, number of IDs, and dispersion and beta function at the ID. A typical scenario without canting results in emittance damping and

\* ilya.agapov@desy.de

Content from this work may be used under the terms of the CC BY 3.0 licence (© 2018). Any distribution of this work must maintain attribution to the author(s), title of the work, publisher, and DOI.

# CURRENT AND FUTURE OF STORAGE RING BASED LIGHT SOURCES IN KEK

N. Higashi\*, K. Harada, T. Honda, Y. Kobayashi, N. Nakamura, KEK, Tsukuba, Japan  
K. Hirano, Hiroshima Univ., Higashi-Hiroshima, Japan

## Abstract

KEK (High Energy Accelerator Research Organization, Tsukuba, Japan) has two storage-ring light sources. One is Photon Factory (PF). This is the first storage-ring light source in X-ray region in Japan, and the user-run started in 1983. The ring energy is 2.5 GeV, and the emittance has been reduced to 36 nmrad from 460 nmrad through some improvements. Another is Photon Factory Advanced Ring (PF-AR). The ring energy is 6.5 GeV, and the single-bunch operation and hard X-ray are featured. The user-run started in 1987, and the emittance is 293 nmrad. The magnetic lattice is almost the same as the original one. Now we consider the future plans of KEK light sources. One is the fully new facility applying DQBA lattice, named KEK-LS. The circumference is 571 m, and the emittance is 315 pmrad @ 3 GeV and 500 mA. In parallel with that, two plans of the only replacements of the lattices reusing existing tunnels of PF and PF-AR are considered. For the PF upgrade, only the arc lattice will be replaced with a new lattice employing combined bends, and the emittance will be improved to 8 nmrad from 35 nmrad. For the PF-AR update, fully replacement will be carried out with a new HMBA lattice, and the expected emittance is 520 pmrad @ 3 GeV and 500 mA.

## PRESENT STATUS

KEK is one of the biggest laboratory in Japan focusing on Accelerator Science, and has not only the high-energy accelerator for the particle experiments but also light sources for the research such as material science and biology. We have two ring-based light source: Photon Factory (PF) and Photon Factory Advanced Ring (PF-AR).

### *Photon Factory*

PF ring began the user operation in 1982 with the horizontal emittance about 460 nm-rad [1,2]. The emittance reduced to about 128 nm-rad by the low emittance configuration in 1986 [3], and about 36 nm-rad by the high-brilliance reconstruction in 1997 [4]. Before the reconstruction in 1997, the normal cell consists of two bending magnets. After the reconstruction, the normal cell consists of only one bending magnet. The number of the quadrupoles, sextupoles and the normal cells were doubled in order to reduce emittance. By the straight sections upgrade in 2005, the lengths of the existing straight sections were extended and new four straight sections for the in-vacuum insertion device were installed. At present, the insertion devices were installed to the all available straight sections.

\* nao.higashi@kek.jp

### *Photon Factory Advanced Ring*

PF-AR is 6.5 GeV light source dedicated to the single bunch operation. The ring originally constructed as an accumulation ring (AR) for TRISTAN project in 1984. Because KEKB, the successor of TRISTAN adopted the full-energy injection from LINAC, AR becomes PF-AR, the full-time synchrotron radiation facility. The circumference of PF-AR is 377 m with four long straight sections. East and west long straight sections are used for RF cavities. North and south straights are originally used for detector development for TRISTAN. Presently, the insertion device is installed in the north straight section and just small accelerator components in south. Because the original injection and extraction systems are installed to the south half of the ring, the experimental hall for SR users are concentrated only in the north half of the ring. The emittance of the present FODO structure lattice is about 300 nmrad for 6.5 GeV that is about two orders of magnitude worse than those of present advanced SR facilities.

## FUTURE PLAN

Now we are planning a construction of a fully-new light source called KEK-LS. This is based on the ESRF-type HMBA (Hybrid Multi Bend Achromat) lattice, and promoted to be constructed in KEK Tsukuba campus. Recently, we improved the design reported in the conceptual design report (CDR) in Oct. 2016 to add the two quadrupole magnets to the short straight section. We call this new lattice DQBA (Double Quadruple Bend Achromat) lattice, and it has more flexibility of the lattice design, better emittance and larger dynamic apertures than the CDR design. In parallel with this, the upgrades for the existing facilities of PF and PF-AR are considered. For the PF upgrade, the limited improvement of the arc part to double the bending magnet and introduce the combined bend will be applied. For the PF-AR upgrade, the full-replacement of the lattice will be carried out employing the flexible DQBA KEK-LS lattice. The scales of the budget and the improvements of the emittance are summarized in Table 1. In the following, the each project is explained in detail.

### *KEK-LS*

KEK-LS is a fourth generation 3.0 GeV light source and promoted to be constructed in KEK Tsukuba campus. We start the lattice design from the example lattice of 3 GeV EBS with 20 cells [5, 6]. Then, the short straight section of 1.2 m was added in order to double the number of the insertion device. We reported this design as CDR [7]. The circumference is about 570 m, and the horizontal natural

Content from this work may be used under the terms of the CC BY 3.0 licence (© 2018). Any distribution of this work must maintain attribution to the author(s), title of the work, publisher, and DOI.

# ACCELERATOR PHYSICS STUDIES FOR THE HIGH ENERGY PHOTON SOURCE IN BEIJING\*

Y. Jiao†, X.H. Cui, Z. Duan, Y.Y. Guo, D.H. Ji, J.Y. Li, X.Y. Li, Y.M. Peng, Q. Qin, S.K. Tian, J.Q. Wang, N. Wang, Y.Y. Wei, G. Xu, H.S. Xu, F. Yan, C.H. Yu, Y.L. Zhao, Key Laboratory of Particle Acceleration Physics and Technology, IHEP, CAS, Beijing 100049, China

## Abstract

The High Energy Photon Source (HEPS) is the next ring-based light source to be built in China, with an emittance of tens of picometers, and a circumference of about 1.3 km. After 10 years' evolution, the design for the HEPS is recently basically determined. In this report we will briefly introduce the latest HEPS lattice design and the progress in related physics studies.

## INTRODUCTION

The High Energy Photon Source (HEPS) is a 6-GeV, 1.3 km, ultralow-emittance storage ring light source to be built in the Huairou District, northeast suburb of Beijing. After iterative discussions, the goal emittance of the HEPS storage ring lattice design is to obtain a natural emittance of below 100 pm.rad.

As the R&D project for HEPS, the HEPS test facility (HEPS-TF) has started in 2016, and is to be completed by the end of Oct., 2018. The goals of the HEPS-TF project are to develop key hardware techniques that are essentially required for constructing a diffraction-limited storage ring light source, and meanwhile, to complete the design for the HEPS project. The main goal of accelerator physics studies is to obtain an 'optimal' lattice design for the HEPS, study the related physics issues and ensure there is no show-stopper from beam dynamics point of view, and give as detailed parameter list and tolerance budget table as possible for various hardware systems.

For the sake of the R&D of key hardware techniques and studies of the related physics issues of the HEPS-TF project, a baseline lattice with 48 identical hybrid-7BAs, a natural emittance of about 60 pm and a large ring acceptance that promises different injection schemes was proposed [1].

For the HEPS project, in 2017, we finished the conceptual design report and the feasibility study report. Now we are preparing the preliminary design report, hoping that we could start the construction before 2019.

Recently, a new lattice with a lower natural emittance, i.e., 34 pm, was proposed for the HEPS project, which still consists of 48 hybrid-7BAs but in 24 periods, and contains superbends and anti-bends.

Based on this lattice, we are carrying out related physics studies, including collective effect study, error effect and lattice calibration simulation, injection system design, injector design, etc. In the following, we will briefly overview the evolution of the lattice design and introduce the status of the related physics studies.

\* Work supported by NSFC (11475202, 11405187, 11205171)

† jiaoyi@ihep.ac.cn

## LATTICE DESIGN & PHYSICS STUDIES

Early in 2008, a kilometre-scale storage ring light source with beam energy of 5 to 6 GeV was proposed to be built in Beijing [2] (called Beijing Advance Photon Source that time). Extensive efforts have been made on the lattice design and related physics studies. As shown in Fig. 1, over the past ten years, the lattice structure has been continuously evolved, from DBA, standard 7BA, TBA, standard 7BA with high-gradient quadrupoles, hybrid 7BA with high-gradient quadrupoles [3-15], to the latest structure, hybrid 7BA with super-bends and anti-bends. The beam energy was fixed to 6 GeV around 2014. The circumference was fixed to 1360.4 m in 2017.

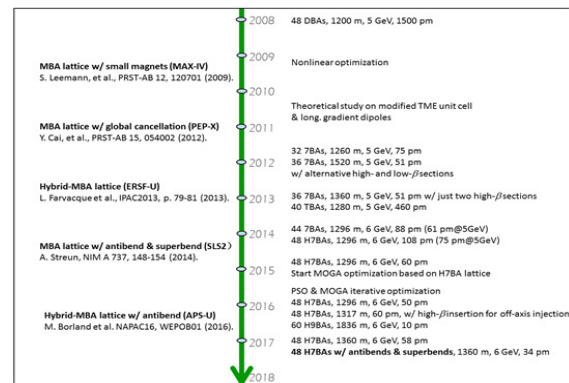


Figure 1: Evolution of the HEPS lattice over the past ten years. The figure also shows several project designs in the world on the left side of the time axis.

Optimization studies [1] based on the HEPS lattice with 48 identical hybrid-7BAs show that there is a trade-off between the emittance (brightness) and the ring acceptance. If satisfying only the dynamic aperture (DA) requirement of on-axis swap-out injection, the HEPS ring emittance can be pushed down to  $\sim 45$  pm.rad; if pursuing large ring acceptance that allows for accumulation injections, the DA can be optimized to be close to (if not larger than) 10 mm in the injection plane, while keeping the emittance to be around 60 pm.rad. The main reason for this trade-off is that the beta function requirements for the DA and brightness optimization are different and even in conflict.

After discussing with beamline experts, we noticed that there are not so many users preferring high brightness as expected. Some users require high flux while not necessarily high brightness. And some users like wide covering range of the synchrotron radiation wavelength, and do not care much about high flux or high brightness. So we decided to look for an alternative high-low beta design. In

# STUDY OF MULTI-BEND ACHROMAT LATTICES FOR THE HALS DIFFRACTION-LIMITED STORAGE RING

Zhenghe Bai<sup>†</sup>, Lin Wang

National Synchrotron Radiation Laboratory, USTC, Hefei 230029, China

## Abstract

In this paper, two multi-bend achromat (MBA) lattice concepts, the locally symmetric MBA and MBA with interleaved dispersion bumps, are described, which have been used to design the Hefei Advanced Light Source (HALS), a soft X-ray diffraction-limited storage ring proposed at NSRL. In these two MBA concepts, most of the nonlinear effects caused by sextupoles can be cancelled out within one lattice cell as in the hybrid MBA proposed by ESRF EBS, but the available family number of sextupoles in one cell can be more than that in the hybrid MBA so that, for example, the tune shift with momentum can be better controlled to increase the dynamic momentum aperture (MA). Using the two MBA concepts, three kinds of lattices, 8BA, 6BA and 7BA, have been studied for the HALS, showing large on- and off-momentum dynamic apertures and large enough dynamic MA.

## INTRODUCTION

Hefei Light Source (HLS) was a second-generation synchrotron light source at NSRL, which was operated in 1991. After about 20 years' operation, HLS started a major upgrade to improve its performance, which was successfully finished in 2014. After the upgrade, the beam emittance was reduced from 160 nm·rad to 40 nm·rad, and the number of the straight sections for insertion devices was increased to 6. Also after the upgrade, a proposal was put forward at NSRL to build a new soft X-ray diffraction-limited storage ring, which was named Hefei Advanced Light Source (HALS). At present, the beam energy of the HALS storage ring is chosen to be 2.4 GeV, and the beam emittance is aimed at less than 50 pm·rad.

The HALS storage ring lattice was initially designed [1] following the main feature of the hybrid multi-bend achromat (MBA) concept proposed by ESRF EBS [2]. But due to the limited families of sextupoles that can be used in one cell, it is hard to increase the dynamic MA. So we considered to develop other MBA concepts, in which not only the nonlinear cancellation can be done within one cell as in the hybrid MBA, but also the family number of sextupoles that can be used in one cell can be more than 3.

## LOCALLY SYMMETRIC MBA LATTICES FOR HALS

In the locally symmetric MBA lattice concept [3], the beta functions of each cell are made locally symmetric about two mirror planes, between which the phase advances satisfy:

$$\mu_x = (2m+1)\pi, \mu_y = n\pi, \quad (1)$$

<sup>†</sup> baizhe@ustc.edu.cn

as shown in Fig. 1. The sextupoles are also placed locally symmetric about the two mirror planes so that most of the nonlinear effects can be cancelled out within one cell, and there can be placed many families of sextupoles in this lattice. According to the position of the midplane in Fig. 1, the locally symmetric MBA can be classified into two kinds. If the midplane is at the middle of the arc section, it is called the first kind; while if the midplane is at the middle of the long straight section, it is called the second kind.

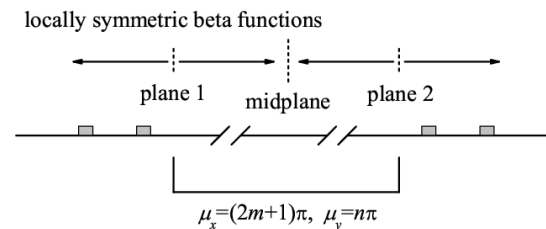


Figure 1: Schematic of locally symmetric MBA lattice.

The locally symmetric MBA of the first kind was used to design an 8BA lattice for the HALS storage ring, and the second kind was used to design a 6BA, which are shown in Fig. 2 and Fig. 3, respectively. Table 1 lists their main parameters. In the 8BA lattice, seven families of sextupoles and one family of octupole were employed for nonlinear dynamics optimization, and the 6BA lattice had five families of sextupoles and two families of octupoles. The nonlinear optimization results of the 8BA lattice with chromaticities corrected to (1, 1) are shown in Fig. 4, Fig. 5 and Fig. 6. The optimized DA is about 150 sigma; the dynamic MA at long straight sections is larger than 7%; and the off-momentum DAs are also large. In addition, from Fig. 5 we can see that if the chromaticities are corrected to slightly higher values, the dynamic MA can be further increased. The nonlinear optimization results of the 6BA lattice are also rather good, see Ref. [3].

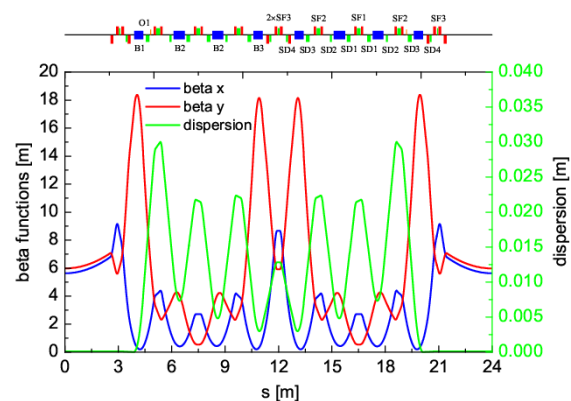


Figure 2: The HALS 8BA lattice.

# MULTI-BEND LATTICE ANALYSIS TOWARDS A DIFFRACTION LIMITED RING BASED LIGHT SOURCE

E. Karantzoulis, Elettra – Sincrotrone Trieste, Italy

## Abstract

An analysis of lattice configurations up to 10 bend achromat is presented aiming towards diffraction limited ring based light source. The described analysis can apply to any type of a ring based light source however for practical reasons we consider Elettra that has been operating for users for 25 years; to stay competitive for world-class photon science in the future, a massive upgrade of the storage ring is needed. The optimum solution is based on certain design criteria, constraints regarding certain accelerator components and their implications on beam dynamics and user requirements. The space available for insertion devices as well as the impact of anti-bends on the design is also addressed. Two proposed realistic lattices are further discussed taking into account different criteria and user requirements. Those lattices reduce the emittance of the present machine by more than one order of magnitude but at the same time respect many other criteria such as realistic magnet gradients, magnets with magnetic length equal to the physical length, drift space enough for radiation extraction, large available space for insertion devices, minimal shift of the beam lines etc.

## INTRODUCTION

Located on the outskirts of Trieste, Elettra operates for users since 1994 being the first third generation light source for soft X-rays in Europe. During those 25 years many improvements have been made to keep the machine competitive with the more modern light sources. At present the Elettra storage ring operates at 2.0 GeV (75% of the user time) and 2.4 GeV (25% of the user time) with beam currents of 310 mA and 160 mA, respectively. The total operating time is about 6400 hours/year of which 5000 are dedicated to the users on a 24/7 basis [1]. The storage ring lattice is a double-bend achromat (DBA) with an emittance of 7 nm-rad at 2 GeV and 10 nm-rad at 2.4 GeV. The ring has a twelve-fold symmetry with 12 long straight sections 11 of which host insertion devices (IDs) most occupying the 4.5 m per achromat pure space available for IDs.

The insertion devices (IDs) include 3 wigglers (one superconducting, one permanent magnet and one electromagnet elliptical) and 8 undulators (3 sections host Apple-II type undulators). Another short undulator is installed in an additional 1.5 m short straight section in the arcs. Ten beam lines use the radiation from six bending magnets to yield the current total of 28 independently operating beam lines. Since 2010, Elettra has been operating in top-up mode, injecting 1 mA of current every 6 / 20 min at 2 GeV / 2.4 GeV, respectively

After 25 years of serving the user community with excellent results, a major upgrade towards what it is called the “ultimate” light source is planned to maintain its leadership for its energy range of synchrotron research and to enable new science and new technology developments to the general benefit.

Following the general trend of the rings for synchrotron light the new generation is generally characterized by a further increase of the brilliance and coherence of the photon source as compared to today’s X-ray beams.

The brilliance of the source in general is given by:

$$B = \frac{\text{flux}}{4\pi^2 \sum_x \sum_{x'} \sum_y \sum_{y'}} \quad (1)$$

and the coherence fraction by:

$$\zeta = \frac{(\lambda / 4\pi)^2}{\sum_x \sum_{x'} \sum_y \sum_{y'}} \quad (2)$$

while the brilliance of the  $n^{\text{th}}$  harmonic of a well matched undulator for the corresponding  $\lambda_n$  photon wavelength is given by:

$$B_n = \frac{F_n}{4\pi^2 (\varepsilon_x + \lambda_n / 2\pi)(\varepsilon_y + \lambda_n / 2\pi)} \quad (3)$$

clearly those quantities become large by further reduction of the emittance of the stored electron beam at levels capable of providing a diffraction limited X-ray source also in the horizontal plane while such a limit has already been achieved at Elettra for the vertical plane. Elettra 2.0 thus, aims to provide intense beams in the range of VUV to X-rays for the analytical study of matter with very high spatial resolution.

Already in the 90’s people were speculating on diffraction limited light sources [2] although the times were not yet ripe. Development in accelerator technologies during the last twenty years led to many important results featuring new magnet design, innovative vacuum and material technologies as well as important improvements in beam monitoring and feedback systems. Those new capabilities and technologies, which were not available or were at their infancy when the present Elettra storage ring was conceived, provide today a solid basis for the realization of the new machine.

Studies being carried out at Elettra resulted in a new storage ring lattice design based on the multi-bend

emanuel.karantzoulis@elettra.eu (2018)

# ION INSTABILITY IN THE HEPS STORAGE RING \*

S.K. Tian<sup>†</sup>, N. Wang

Key Laboratory of Particle Acceleration Physics and Technology, Institute of High Energy Physics, Chinese Academy of Sciences, 100049 Beijing, China

## Abstract

Ionisation of residual gases in the vacuum chamber of an accelerator will create positively charged ions. For the diffraction limit storage ring, the ion effect has been recognized as one of the very high priorities of the R&D for the High Energy Photon Source (HEPS), due to the ultra-low beam emittance and very high intensity beam. In this paper, we have performed a simulation based on the weak-strong model and analytical estimate to investigate characteristic phenomena of the fast-ion instability.

## INTRODUCTION

The ionization of the residual gas in the vacuum pipe by the circulating electron beam will create positive ions. These ions could be trapped in the potential well of the stored beam under certain conditions [1]. The accumulation depends on several factors, e.g. the filling pattern (the number of bunches, bunch spacing, beam current), transverse beam sizes (beam emittances, the storage ring optics) and the property of the ions (the mass, the charge).

Generally speaking, ion effects can be divided into two categories. One is called conventional ion trapping instability and the other is called fast beam-ion instability (FBII) [2, 3]. The former occurs mainly in the storage rings when bunches are uniformly filled. If some conditions are satisfied, the ions are accumulated over many turns and trapped by the beam potential all the time. These ions mutually couple to the motion of beam particles and lead to a beam instability in the ring. This instability can be partially suppressed by intentionally leaving a gap after the bunch train. These gaps will make the ions over focused and eventually lost to the vacuum chamber wall [4]. However, the diffraction limit storage ring light source feature an extremely small beam emittance (nanometer scale) and many bunches (a few hundreds) operation. The bunch spacing is therefore not very long enough, single passage ion instability, which is called fast beam-ion instability, is dominant. In this case, ions created by the head of the train via ionization of the residual gas perturb the tail during the passage of a single electron bunch train.

The High Energy Photon Source (HEPS), a kilometre scale quasi-diffraction limited storage ring light source with the beam energy of 6 GeV, is to be built in Beijing area and now is under extensive design. Extensive efforts have been made on the lattice design and relevant studies of this project. A hybrid 7BA design for the HEPS has been made. The design beam current is 200 mA, and basically two filling patterns are under consideration. One is the high

brightness mode with 680 bunches (1.3nC, 0.3mA), followed by a 10% gap; the other one is the timing mode, with 63 bunches (14.4nC, 3.2mA) of equal bunch charges uniformly distributed around the ring. The main parameters were listed in Table 1.

Table 1: HEPS Lattice Design Parameters

Parameters	Values
Energy $E_0$	6 GeV
Beam current $I_0$	200 mA
Circumference	1360.4 m
Natural emittance $\epsilon_{x0}$	58.4 pm.rad
Working point $\nu_x/\nu_y$	107.37/82.43
Natural chromaticity (H/V)	-214/-133
No. of super-periods	48
ID section length $L_{ID}$	6.15m
RMS energy spread	$8.20 \times 10^{-4}$
Momentum compaction	$3.43 \times 10^{-5}$
Energy loss per turn	1.959 MeV

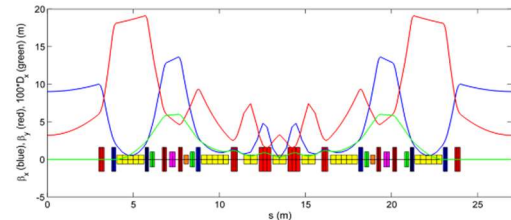


Figure 1: Optical functions and lattice structure for one cell of the HEPS storage ring.

## ION TRAPPING

The ions generated by beam-gas ionization will experience a force from the passing electron bunch, which can be regarded as a thin lens focusing element followed by a drift space before the next bunch passes. Based on the linear theory of ion trapping [5], the ions with a relative molecular mass greater than  $A_{x,y}$  will be trapped horizontally (vertically) in the potential well of the beam. The  $A_{x,y}$  in units of amu is given by:

$$A_{x,y}(s) = \frac{N_e r_p L_{sep}}{2(\sigma_x(s) + \sigma_y(s))\sigma_{x,y}}, \quad (1)$$

Where  $N_e$  is the number of particles per bunch,  $r_p$  ( $\sim 1.535 \times 10^{-18}$ m) is the classical proton radius,  $L_{sep}$  is the bunch separation in meters,  $\sigma_x(s)$ , is the local horizontal rms beam size, and  $\sigma_y(s)$  is the local vertical rms beam size.

The ions should be trapped both in x and y directions simultaneously, so the critical mass in units of amu is given by:

$$A_{crit}(s) = \frac{N_e r_p L_{sep}}{2 \min(\sigma_x(s), \sigma_y(s))(\sigma_x(s) + \sigma_y(s))}. \quad (2)$$

\* Work supported by NSFC (11475202, 11405187, 11205171)

<sup>†</sup> tiansk@ihep.ac.cn

# A STUDY ON THE IMPROVED CAVITY BUNCH LENGTH MONITOR FOR FEL\*

Q. Wang, Q. Luo<sup>†</sup>, B. G. Sun<sup>‡</sup>, Y. L. Yang, Z. R. Zhou, P. Lu, F. F. Wu, L. L. Tang, T. Y. Zhou,  
 X. Y. Liu, J. H. Wei,

NSRL, University of Science and Technology of China,  
 230029 Hefei, P. R. China

## Abstract

Bunch length monitors based on cavities have great potential especially for future high quality beam sources because of many advantages such as simple structure, wide application range, and high signal-to-noise ratio (SNR). The traditional way to measure bunch length needs two cavities at least. One is reference cavity, whose function is to get the beam intensity. The other one is defined as main cavity, which is used to calculate the bunch length. There are some drawbacks. To improve performance, the mode and the cavity shape are changed. At the same time, the position and orientation of coaxial probe are designed to avoid interference modes which come from the cavity and beam tube according to the analytic formula of the electromagnetic field distribution. A series simulation based on CST is performed to verify the feasibility, and the simulation results reveal that the improved monitor shows good performance in bunch length measurement.

## INTRODUCTION

Bunch length is one of the main characteristics of charged particle beam in accelerator. There is growing interest in the generation, measurement and application of short electron bunches, so precise bunch length measurement methods are necessary for developing the future light sources. To measure the bunch length, many methods have been developed in the past decades. Bunch length monitor based on cavities has great potential especially for high quality beam sources because of many advantages such as simple structure, wide application range, and high signal noise ratio. What's more, the cavities with different modes show the ability of combined measurement of bunch length, beam intensity, position and quadrupole moment so that the whole diagnostic system is simplified and compact. In this paper, a series of studies about improved cavity bunch length monitors for the National Synchrotron Radiation Laboratory Infrared Free Electron Laser (FELiChEM) are presented. The beam parameters, used in the analytical calculation and simulation of this paper, are listed in Table 1.

\* Supported by The National Key Research and Development Program of China (Grant No. 2016YFA0401900, 2016YFA0401903), the National Science Foundation of China (Grant No. 11375178, 11575181) and the Fundamental Research Funds for the Central Universities (WK2310000046).

<sup>†</sup> luoqing@ustc.edu.cn  
<sup>‡</sup> bgsun@ustc.edu.cn

Table 1: Electron Beam Parameters of IR-FEL

Parameter	Value
Beam energy	30~50 MeV
Bunch charge	1 nC
Bunch length, rms	2~5 ps
Bunch repetition rate	476 MHz
Beam pipe radius	17.5 mm
Macro pulse length	13 $\mu$ s
Macro pulse repetition rate	10 Hz

## THEORETICAL BASIS

Cavity bunch length monitor is usually composed of two cavities with different working frequencies. When a Gaussian bunch passed through the axis of the vacuum chamber, the symmetric TM<sub>0n0</sub> modes could be excited in the cavities. The power of one mode can be written as [1].

$$\begin{cases} P_1 = [I_0 \exp(-\frac{\omega_1^2 \sigma_\tau^2}{2})]^2 R_1 \\ P_2 = [I_0 \exp(-\frac{\omega_2^2 \sigma_\tau^2}{2})]^2 R_2 \end{cases} \quad (1)$$

Where the subscripts stand for the cavities' serial number,  $\sigma_\tau$  is the bunch length,  $I_0$  is pulse current,  $\omega$  is resonance frequency of the mode, and  $R$  is cavity shunt impedance. The  $\sigma_\tau$  and  $I_0$  are quantified by solving this two simultaneous power equations.

## DESIGN IMPROVEMENTS

### Design of the System

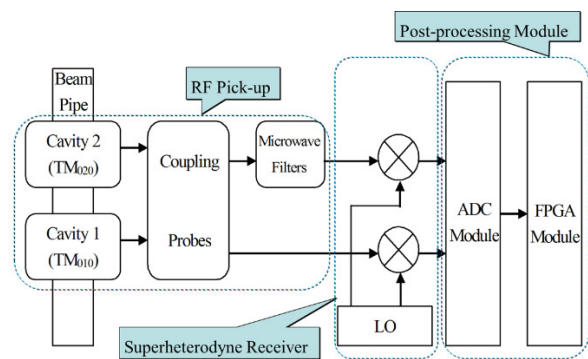


Figure 1: The schematic diagram of a single cavity.

The framework of the whole diagnostic system is shown in Fig. 1. The RF pick-up is composed of two cav-

# THE DEVELOPMENT AND APPLICATIONS OF THE DIGITAL BPM SIGNAL PROCESSOR AT SINAP\*

L.W. Lai<sup>†</sup>, Y.B. Leng, Y.B. Yan, W.M. Zhou, F.Z. Chen, J. Chen, S.S. Cao,  
 SSRF, SINAP, Shanghai, China

## Abstract

A Digital BPM signal processor has been designed in SINAP since 2009. It is a general platform that can be used for the signal processing of a variety of BPM, like stripline BPM, cavity BPM and button BPM. After years of optimization, the DBPM has been used massively on DCLS and SXFEL. And the turn-by-turn resolution of the storage ring DBPM on SSRF is 0.34 $\mu$ m. This topic will introduce the development and applications of the DBPM at SINAP, also the future DBPM development for next generation light source will be discussed here.

## INTRODUCTION

BPM is an important diagnostic instrument in accelerator. It provides the beam position in tunnel, which can be used for accurate beam control and other beam parameters measurements. There have a variety of BPM sensors for different occasions on accelerator, such as stripline BPM, button BPM, cavity BPM, shoebox BPM, et.al. Except for the sensor, the BPM signal processing electronic is a key component of the BPM system. The signal processing system can mainly including RF signal conditioning, ADCs digitizing analogue signal into digital signal, FPGA processing digital signal and calculate the beam position, data acquisition in CPU sending out the results and communicating with control center through LAN. Figure 1 is the block diagram of BPM signal processing system.

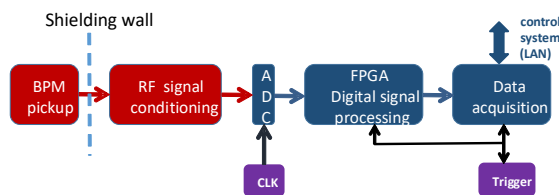


Figure 1: BPM signal processing system.

BPM sensors are installed at the concerned place of the accelerator, larger accelerator always containing more BPMs. For example SSRF is a 432m electron storage ring and contains about 200 BPMs, and future Shanghai Hard X-ray FEL will have more than 200 BPMs along the 3km facility. Since 2009, SSRF started the development of DBPM processor, the objective is to develop a stand-alone

general hardware platform that can be used for diverse signal processing applications on accelerator. The first version DBPM completed at about 2011, and lab-tests and on-line beam tests have been carried out. The results shown that the turn-by-turn data resolution can be better than 1 $\mu$ m, and the 10Hz SA data can be read correctly [1]. After five years' optimization, a second version DBPM has been designed and firstly made mass field application on DCLS and SXFEL, and small amount DBPMs is under test on SSRF.

The DBPM specification is listed in Table 1.

Table 1: DBPM Specifications

Parameter	Value
Channels	4
Central Frequency	500MHz
Bandwidth	~20MHz
Dynamic range	31dB
ADC bits	16
ADC bandwidth	650MHz
Max ADC rate	125MSPS
FPGA	Xilinx xc5vsx50t
Clock	Ext./Int.
Trigger	Ext./Self/Period
Software	Arm-Linux/EPICS

Figure 2 is the architecture of the processor. RF conditioning and ADCs are located on RF board, others on digital carrier board. Figure 3 is the hardware of RF board and digital board.

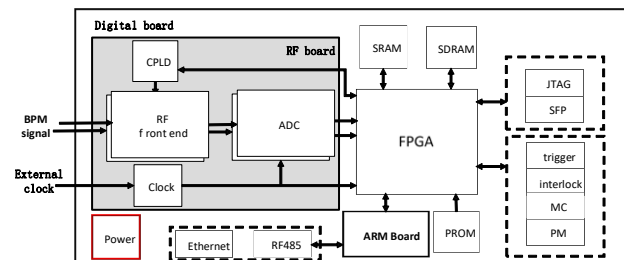


Figure 2: Processor architecture.

\*Supported by The National Science Foundation of China (Grant No.11305253, 11375255, 11575282); The National Key Research and Development Program of China (Grant No. 2016YFA0401990, 2016YFA0401903).

<sup>†</sup> lailongwei@sinap.ac.cn

# TURN-BY-TURN MEASUREMENTS FOR SYSTEMATIC INVESTIGATIONS OF THE MICRO-BUNCHING INSTABILITY\*

J. L. Steinmann<sup>†</sup>, M. Brosi, E. Bründermann, M. Caselle, S. Funkner, B. Kehrer,  
 M. J. Nasse, G. Niehues, L. Rota, P. Schönfeldt, M. Schuh, M. Siegel, M. Weber and A.-S. Müller  
 Karlsruhe Institute of Technology, Karlsruhe, Germany

## Abstract

While recent diffraction-limited storage rings provide bunches with transverse dimensions smaller than the wavelength of the observed synchrotron radiation, the bunch compression in the longitudinal plane is still challenging. The benefit would be single cycle pulses of coherent radiation with many orders of magnitude higher intensity. However, the self-interaction of a short electron bunch with its emitted coherent radiation can lead to micro-bunching instabilities. This effect limits the bunch compression in storage rings currently to the picosecond range. In that range, the bunches emit coherent THz radiation corresponding to their bunch length. In this paper, new measurement setups developed at the Karlsruhe Institute of Technology are described for systematic turn-by-turn investigations of the micro-bunching instability. They lead to a better understanding thereof and enable appropriate observation methods in future efforts of controlling and mastering the instability. Furthermore, the described setups might also be used as high repetition rate bunch compression monitors for bunches of picosecond length and below.

## MICRO-BUNCHING INSTABILITY

The micro-bunching instability (MBI) is a longitudinal instability that arises due to the self-interaction of a bunch with its emitted electro-magnetic field<sup>1</sup>. This interaction can be modelled by a synchrotron-radiation impedance whose real part corresponds to the emitted radiation. The impedance has a low frequency cutoff due to the shielding of the vacuum chamber [2] and a high frequency cutoff due to the particle energy. The shielded wavelengths can be approximated with the shielding cutoff  $\lambda = 2h\sqrt{h/R}$  with  $h$  being the beam pipe height and  $R$  the particles radius of curvature, while the high frequency cutoff can be approximated by the critical frequency of the synchrotron radiation  $f_c = 3\gamma^3 c / (4\pi R)$ . Therefore, the impedance has significant strength if  $\gamma^3 \sqrt{h^3 R^{-3}} \gtrsim 2$ . While this applies to almost all light sources, only a few heavy particle machines reach high enough energies. However, also future colliders will be confronted with high amount of synchrotron radiation.

In order to generate a significant wake potential, the bunch spectrum and the impedance need to overlap. As a rule

of thumb, storage rings with a few meters bending radius and some tens of centimeters beam-pipe height typically have a cutoff around hundred gigahertz, leading to a critical bunch length around ten picoseconds. At first, the additional wake potential leads to potential well distortion and a change of bunch shape. Then, above a critical bunch charge, a self-amplified system is formed since the distorted bunch shape increases the wake potential further. This leads to the formation of sub-structures on the bunch profile and a blow-up of the bunch in phase space. The blow-up is much faster and stronger than the damping time and no equilibrium is reached. The bunch is blown up, until the wake potential becomes negligible. Then, the radiation damping shortens the bunch, until the threshold is hit again. Consequently, a sawtooth behaviour is observed.

Due to the characteristic bunch size of a few picoseconds and even smaller substructures, signatures of the instability can be seen in the terahertz frequency range where outbursts of coherent radiation are observed. Obviously, the behaviour is beam current dependent, too.

The relevant time scales when observing the MBI reach from a few turns during the start of a burst, over some milliseconds between consecutive bursts, to minutes and hours when analyzing current dependent changes. Consequently, the diagnostics need to be single shot, turn-by-turn and be able to record for long time scales. In this paper, we will present recent diagnostic systems developed and evaluated at the Karlsruhe Institute of Technology (KIT).

## KARLSRUHE RESEARCH ACCELERATOR

The Karlsruhe Research Accelerator (KARA) is the 2.5 GeV storage ring of the KIT. It can be varied for a broad range of parameters (see Table 1). A special short-bunch mode is established at 1.3 GeV.

Table 1: KARA Parameters

L	110.4	m
$f_{RF}$	499.7	MHz
h	32	mm
Energy	0.5 to 2.5	GeV
$V_{RF}$	150 to 1500	kV
$\alpha_c$	$1.6 \times 10^{-4}$ to $1 \times 10^{-2}$	
$\sigma_{z,0}$	1.9 to 45	ps

\* Funded by the German Federal Ministry of Education and Research (Grant No. 05K16VKA) & Initiative and Networking Fund of the Helmholtz Association (contract number: VH-NG-320). M. Brosi, P. Schönfeldt and J. Steinmann acknowledge the support of the Helmholtz International Research School for Teratronics (HIRST).

<sup>†</sup> johannes.steinmann@kit.edu

<sup>1</sup> For a good summary of the topic see Ref. [1].

Content from this work may be used under the terms of the CC BY 3.0 licence (© 2018). Any distribution of this work must maintain attribution to the author(s), title of the work, publisher, and DOI.

# PRELIMINARY DESIGN OF HEPS STORAGE RING VACUUM CHAMBERS AND COMPONENTS

P. He, B.L. Deng, D.Z. Guo, Y.S. Ma, B.Q. Liu, Q. Li, Y.C. Yang, L. Zhang, X.J. Wang,  
 Institute of High Energy Physics, CAS, Beijing, P.R. China

## Abstract

The 4<sup>th</sup> generation ring-based light sources, HEPS (High Energy Photon Source) 7BA lattice has been developed at IHEP. This is 6Gev, 200mA machine which has horizontal emittance  $\epsilon_h$  around 60pm.rad to gain the high brilliance photon beam. This compact lattice bring the magnet aperture to 25mm diameter, this will place a demanding set of constraints on the storage ring vacuum system design. Hybrid design has been adopted this lattice which combines conventional chambers incorporating “antechambers” with a variety of simpler tubular chambers made variously of copper-plated stainless steel, and NEG-coated copper tube in the FODO section.

## INTRODUCTION

The main issues of low emittance ring vacuum system are providing the effective pumping and handling the higher SR power. The general requirements for vacuum chamber have to be considered for the cost, performance, and required maintenance, these factors will led to a design by which the details of the chamber construction varies according to local spatial constraints and SR loading. The next-generation light source storage ring vacuum system has to be designed in such way which is compatible with a multi-bend achromat(MBA) compact lattice [1]. Three different approaches have been developed: Conventional chamber with antechamber [2], all NEG-coated copper tubes [3], and hybrid design which combines conventional chambers and tubular NEG-coated copper tube [4]. For the HEPS storage ring vacuum system, we choose the hybrid design. This option takes both advantage of type I and type II design, it has good vacuum performance and reduce the vacuum chamber impedance, and also can shorter the required installation time, and easy maintainability. Also the system cost is at the moderate level.

## SYSTEM DESIGN

As presently envisioned, a 7BA lattice storage ring will store 200 mA of electron current at an energy of 6 GeV for HEPS. One cell layout of the storage ring is shown in Fig. 1. According to the difference of the magnet function, the sector is divided into four types of sections: quadrupole doublet, longitudinal gradient dipole, multipole straight, FODO (alternately of focusing and defocusing). Vacuum chamber cross-section and material selection will depend on the synchrotron radiation power distribution there and also need integrate with other components(magnet, BPM, et al.). The issues such as space between magnet pole tips, coil gaps for vacuum and photon extraction chambers, all of these need to be consid-

ered when we design the vacuum chamber. The different vacuum chamber design will be presented as below.

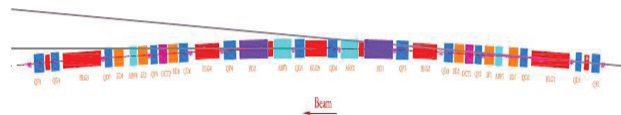


Figure 1: One sector of HEPS lattice layout.

## Quadrupole Doublet Chamber

In this section, the fast corrector magnet is located between two quadrupoles, the Inconel segment will be used on this area to limit the impact of eddy current shielding by increasing electrical resistivity ( $7.4 \times 10^{-7} \Omega \cdot m \rightarrow 1.28 \times 10^{-6} \Omega \cdot m$ , 40% higher compare with 316LN stainless steel).

The interior surface, however, will be plated with copper to minimize beam impedance effects. The chamber layout is shown at Fig. 2.

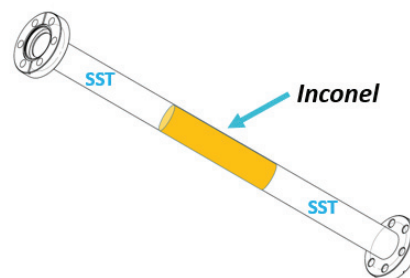


Figure 2: Quadrupole doublet chamber with Inconel segment.

## LGD Chamber (Longitudinal Gradient Dipole)

Chambers here will have a 22 mm aperture for the particle beam and antechambers to allow discrete absorbers to intercept bending magnet radiation away from the stored beam (Fig. 3). In order to provide the good vacuum performance, two NEG pump will be add to the antechamber side. Finite element analysis (FEA) was used to calculate the mechanical stresses in vacuum chamber. The primary results show the max. deformation is 0.055mm and max. stress is 17.8MPa, the further optimization of the design still underway.

## Straight Multiplet Chamber and X-ray Extraction Chamber

The ray trace simulation indicate that the very less bending magnet radiation shooting on the chamber wall in the straight multiplet section even without antechamber and just very simple tubular chamber. The key-hole chamber is applied here for the x-ray extraction which

# TRANSPORTATION AND MANIPULATION OF A LASER PLASMA ACCELERATION BEAM\*

A. Ghaith<sup>†</sup>, T. André, A. Loulergue, M. Labat, D. Oumbarek, C. Kitegi, I. Andriyash, F. Briquez, M. Valléau, F. Marteau, O. Marcouillé, F. Blache, F. Bouvet, Y. Dietrich, J. P. Duval, M. El-Ajjouri, C. Herbeaux, N. Hubert, N. Leclercq, A. Lestrade, P. Rommeluere, M. Sebdaoui, K. Tavakoli, M. E. Couprie, Synchrotron SOLEIL, GIF-sur-YVETTE, France  
 C. Thaury, G. Lambert, S. Corde, J. Gautier, B. Mahieu, K. Ta Phuoc, V. Malka, Laboratoire d'Optique Appliquée, Orsay, France  
 E. Roussel, Bielawski, C. Evain, C. Szwaj, Laboratoire PhLAM, Lille, France

## Abstract

The ERC Advanced Grant COXINEL aims at demonstrating free electron laser amplification, at a resonant wavelength of 200 nm, based on a laser plasma acceleration source. To achieve the amplification, a 8 m long dedicated transport line was designed to manipulate the beam qualities. It starts with a triplet of permanent magnet with tunable gradient quadrupoles (QUAPEVA) that handles the highly divergent electron beam, a demixing chicane with a slit to reduce the energy spread per slice, and a set of electromagnetic quadrupoles to provide a chromatic focusing in a 2 m long cryogenic undulator. Electrons of energy 176 MeV were successfully transported throughout the line, where the beam positioning and dispersion were controlled efficiently thanks to a specific beam based alignment method, as well as the energy range by varying the slit width. Observations of undulator radiation for different undulator gaps are reported.

## INTRODUCTION

Laser Plasma Acceleration (LPA) [1–3] has proven to be an efficient way to produce high energy electrons within a short accelerating distance. It can produce a GeV electron beam within a distance of few cms [4], high peak current up to 10 kA and short bunch length (few fs). However, the divergence is quite high of the order of few mrad and so is the energy spread (few %) [5]. A powerful laser focused on a gas chamber ionizes the gas molecules and pushes the electrons out of its path leaving the ions un-affected. This induces a plasma wave with an intense electric field following the direction of the laser. The electron beam caught in between the laser pulse and the plasma wave is accelerated until it surpasses the wave and thus attains maximum energy possible.

Undulator radiation has been successively observed [6–10] using LPA source, while Free Electron Laser (FEL) based applications remain very challenging due to the beam quality that does not fit the FEL requirements:

$$\begin{cases} \epsilon_N < \frac{\gamma\lambda}{4\pi} \\ \sigma_\gamma < \rho \end{cases} \quad (1)$$

where  $\epsilon_N$  is the normalized emittance,  $\gamma$  the Lorentz factor,  $\lambda$  the radiation wavelength to be amplified,  $\sigma_\gamma$  the energy spread (FWHM) and  $\rho$  the pierce parameter:

$$\rho = \left[ \frac{1}{16} \frac{I_{peak}}{I_A} \frac{\lambda_u^2 K^2 [JJ]^2}{4\pi^2 \gamma^2 \sigma_x \sigma_z} \right]^{1/3} \quad (2)$$

where  $I_{peak}$  is the peak current,  $I_A$  the Alfven current (17 kA),  $\lambda_u$  the undulator magnetic period,  $K$  the deflection parameter proportional to the undulator peak field and period,  $[JJ] = J_0(\kappa) - J_1(\kappa)$  ( $\kappa = \frac{K^2}{4+2K^2}$ ),  $\sigma_x$  and  $\sigma_z$  are the horizontal and vertical beam size (rms) respectively.

COXINEL [11–19], among other LPA based projects [20, 21], aims at demonstrating FEL amplification by the help of a dedicated transport line to handle and manipulate the beam properties [22].

## BEAM MANIPULATION LINE

The line starts by focusing an intense Sa:Ti laser (800 nm) with 30 TW power, 1.5 mJ energy and 30 fs pulse duration on a gas jet composed of 99% He and 1% N<sub>2</sub>. The baseline reference case of the slice beam parameters produced are shown in Table 1 (source). High gradient quadrupoles (~200 T/m) are used to decrease the beam divergence, and a chicane accompanied with a slit to select the desired energy. Table 1 (undulator) presents the electron beam parameters after beam manipulation. The divergence is reduced by a factor of 10 with a beam size of 50 μm corresponding to a normalized emittance of 1.7 mm.mrad that satisfy the first FEL condition. The slice energy spread is reduced by a factor of 10 on the expense of the peak current where the beam is decompressed (longer bunch length). Thus FEL amplification is feasible after such manipulation.

\* Work supported by SOLEIL

<sup>†</sup> amin.ghaith@synchrotron-soleil.fr

# 'LWFA-DRIVEN' FREE ELECTRON LASER FOR ELI-BEAMLINES

A.Y. Molodozhentsev\*, G. Korn, L. Pribyl, ELI-BL, Institute of Physics of CAS,  
Prague, Czech Republic

A.R. Maier, University of Hamburg and CFEL, Hamburg, Germany

## Abstract

Free-electron lasers (FEL) are unique light source for different applications on the femto-second scale, including for instance studying of the most basic reaction mechanisms in chemistry, structural biology and condense physics. Laser wake field acceleration (LWFA) mechanism allows to produce extremely short electron bunches of a few-fs length with the energy up to a few GeV providing peak current of many kA in extremely compact geometries. This novel acceleration method therefore opens a new way to develop compact "laser-based" FEL. ELI-beamlines (ELI-BL) is an international user facility for fundamental and applied research using ultra-intense lasers and ultra-short high-energy electron beams. In frame of this report we present conceptual solutions for an electron beam transport of a compact "LFWA" based soft X-ray FEL, which can deliver a photon peak brightness up to  $10^{31}$  photons/sec/mm<sup>2</sup>/mrad<sup>2</sup>/0.1%BW. A combination of this achievement with novel laser technologies will open a new perspective for the development of extremely compact FELs with few or even sub-femtosecond photon bunches for a very wide user community.

## INTRODUCTION

A few years ago, a new type of large-scale laser infrastructure specifically designed to provide high peak power and focused intensity ultrashort pulses was heralded by the European Community: the Extreme Light Infrastructure (ELI) [1]. ELI will be the world's first international laser research infrastructure. ELI is implemented as a distributed research infrastructure based on 3 specialized and complementary facilities located in the Czech Republic, Hungary and Romania. ELI-beamlines (near Prague, the Czech Republic) will be the high-energy beam facility responsible for development and use of ultra-short pulses of high-energy particles and radiation stemming from the ultra-relativistic interaction. Using laser systems in ELI-BL it will be possible to accelerate electrons up to a few GeV.

The principle of the 'laser-wake-field-acceleration' (LWFA) [2] is based on an ultra-high longitudinal electric gradient, created by the high-intensity laser pulse focused in dense plasma (in a gas-jet, gas-cell or capillary discharge targets). The ponderomotive force pushes the plasma electrons out of the laser beam path, separating them from the ions. A travelling longitudinal electric field can reach several hundreds of GV/m, which is much larger than the accelerating field achievable in conventional accelerators, making LWFA extremely attractive as a compact accelerator to provide high-energy beams for

different applications. During last decades, a remarkable progress has been made in the field of electron acceleration based on the LWFA concept. Electron beams with peak energies of multi-GeV have been obtained experimentally [3]. However, a controllable high-quality electron beam with desirable properties such as energy spread, low emittance, small transverse divergence and large beam charge are not demonstrated using a single-stage LWFA setup up to now. Remarkable experimental achievement has been reached recently using a cascaded acceleration [4] of electrons by decoupling the injection and acceleration. Through manipulating electron injection, quasi-phase-stable acceleration, electron seeding in different periods of the wake-field, as well as controlling the energy chirp, the high-quality electron beams have been obtained. The electron beams with energies in the range of 200÷600MeV, with the RMS energy spread of 0.4÷1.2%, the RMS transverse beam divergence of 0.2mrad with the bunch charge of 10÷80pC have been demonstrated experimentally for this new cascaded acceleration scheme [5].

Using recent experimental achievements one can define the parameters of the LWFA electron beam at the exit of the plasma channel as following: the electron beam energy in the range from 300MeV to 1000MeV; the RMS transverse beam size in the horizontal and vertical plane is 1μm or less; the RMS transverse beam divergence in the horizontal and vertical planes is 0.5mrad or less; the RMS bunch length is about 1μm; the RMS relative (total) energy spread is less than 1%; the normalized RMS transverse beam emittance in the horizontal and vertical planes is  $0.2\pi$  mm.mrad; the bunch charge is about 20÷50pC. In frame of this report we discuss a conceptual solution for a dedicated electron beamline to transport high-energy electrons from a plasma target up to an undulator for a 'demonstration' FEL experiment with a possible expansion of such beamline to use it for a 'laser-driven' FEL, which is under discussion now in the ELI-BL Center.

Uniqueness of the 'laser-driven' FEL is based on the laser properties. The laser pulse of a few tens of fs allows to produce extremely short electron bunch with the bunch duration of a few fs. Such short electron bunch passing through an undulator magnetic field can produce a 'single-spike' coherent photon radiation, if FEL resonance conditions are satisfied. In principle, the 'laser-driven' FEL can operate with high repetition rate (up to 100Hz), which is limited by the current 'state-of-art' of the laser technology.

\* Correspond. author: Alexander.Molodozhentsev@eli-beams.eu

# HARMONIC LASING IN X-RAY FELS: THEORY AND EXPERIMENT

E. A. Schneidmiller\*, B. Faatz, M. Kuhlmann, J. Rönsch-Schulenburg,  
 S. Schreiber, M. Tischer, M. V. Yurkov

Deutsches Elektronen-Synchrotron (DESY), Notkestrasse 85, D-22607 Hamburg, Germany

## Abstract

Harmonic lasing is a perspective mode of operation of X-ray FEL user facilities that allows to provide brilliant beams of higher energy photons for user experiments. Another useful application of harmonic lasing is so called Harmonic Lasing Self-Seeded Free Electron Laser (HLSS FEL) that allows to improve spectral brightness of these facilities. In the past, harmonic lasing has been demonstrated in the FEL oscillators in infrared and visible wavelength ranges, but not in high-gain FELs and not at short wavelengths. In this paper we report on the first evidence of the harmonic lasing and the first operation of the HLSS FEL at the soft X-ray FEL user facility FLASH in the wavelength range between 4.5 nm and 15 nm.

## INTRODUCTION

Successful operation of X-ray free electron lasers (FELs) [1–3], based on self-amplified spontaneous emission (SASE) principle [4], down to an Ångström regime opens up new horizons for photon science. Even shorter wavelengths are requested by the scientific community.

One of the most promising ways to extend the photon energy range of high-gain X-ray FELs is to use harmonic lasing which is the FEL instability at an odd harmonic of the planar undulator [5–9] developing independently from the lasing at the fundamental. Contrary to the nonlinear harmonic generation [1, 6, 7, 10–13] (which is driven by the fundamental in the vicinity of saturation), harmonic lasing can provide much more intense, stable, and narrow-band radiation if the fundamental is suppressed. The most attractive feature of saturated harmonic lasing is that the spectral brightness of a harmonic is comparable to that of the fundamental [9].

Another interesting option, proposed in [9], is the possibility to improve spectral brightness of an X-ray FEL by the combined lasing on a harmonic in the first part of the undulator (with an increased undulator parameter  $K$ ) and on the fundamental in the second part of the undulator. Later this concept was named Harmonic Lasing Self-Seeded FEL (HLSS FEL) [14]. Even though this scheme is not expected to provide an ultimate monochromatization of the FEL radiation as do self-seeding schemes using optical elements [15–17], it has other advantages that we briefly discuss below in the paper.

Harmonic lasing was initially proposed for FEL oscillators [18] and was tested experimentally in infrared and visible wavelength ranges [19–22]. It was, however, never demonstrated in high-gain FELs and at a short wavelength.

In this paper we present the first successful demonstration of this effect at the second branch of the soft X-ray FEL user facility FLASH [23] where we managed to run HLSS FEL in the wavelength range between 4.5 nm and 15 nm.

## HARMONIC LASING

Harmonic lasing in single-pass high-gain FELs [5–9] is the amplification process of higher odd harmonics developing independently of each other (and of the fundamental harmonic) in the exponential gain regime. In the case of a SASE FEL the fluctuations of the beam current with frequency components in the vicinity of a wavelength

$$\lambda_h = \frac{\lambda_w(1 + K^2)}{2h\gamma^2} \quad h = 1, 3, 5 \dots \quad (1)$$

serve as an input signal for amplification process. Here  $\lambda_w$  is the undulator period,  $\gamma$  is relativistic factor,  $h$  is harmonic number, and  $K$  is the rms undulator parameter:

$$K = 0.934 \lambda_w[\text{cm}] B_{\text{rms}}[\text{T}],$$

$B_{\text{rms}}$  being the rms undulator field (peak field divided by  $\sqrt{2}$  for a planar undulator with the sinusoidal field).

An advantage of harmonic lasing over lasing on the fundamental at the same wavelength can be demonstrated for the case of a gap-tunable undulator. In this case one uses a higher  $K$ -value for harmonic lasing, i.e. for the lasing on the fundamental one has to reduce  $K$  to the value  $K_{re}$ :

$$K_{re}^2 = \frac{1 + K^2}{h} - 1. \quad (2)$$

Obviously,  $K$  must be larger than  $\sqrt{h-1}$ .

Then one can derive a ratio of the gain length of the fundamental,  $L_g^{(1)}$ , to the gain length of a harmonic  $L_g^{(h)}$  [9]:

$$\frac{L_g^{(1)}}{L_g^{(h)}} = \frac{h^{1/2} K A_{JJh}(K)}{K_{re} A_{JJ1}(K_{re})}. \quad (3)$$

Here  $A_{JJh}(K) = J_{(h-1)/2} \left( \frac{hK^2}{2(1+K^2)} \right) - J_{(h+1)/2} \left( \frac{hK^2}{2(1+K^2)} \right)$  is the coupling factor for harmonics with  $J_n$  being Bessel functions.

The formula (3) is obtained in the frame of the three-dimensional theory including diffraction of the radiation, emittance, betatron motion (and for an optimized beta-function) but assuming a negligible energy spread. The plot of the ratio of gain lengths (3) is presented in Fig. 1. It is clearly seen that harmonic lasing has always a shorter gain length under above mentioned conditions (and the ratio is larger than that obtained in one-dimensional model [8]). The ratio shown in Fig. 2 starts to diverge rapidly for the

\* evgeny.schneidmiller@desy.de

# DIELECTRIC AND OTHER NON-PLASMA ACCELERATOR BASED COMPACT LIGHT SOURCES\*

R. J. England<sup>†</sup>, Z. Huang

SLAC National Accelerator Laboratory, Menlo Park, CA 94025, USA

## Abstract

We review recent experimental progress in developing nanofabricated dielectric laser-driven accelerators and discuss the possibility of utilizing the unique sub-femtosecond electron pulse format these accelerators would provide to create ultra-compact EUV and X-ray radiation sources.

## INTRODUCTION

Particle acceleration in dielectric structures driven by ultrafast infrared lasers, a technique we refer to as “dielectric laser acceleration” (DLA), is a new and rapidly progressing area of advanced accelerator research that sets the stage for future generations of high-gradient accelerators of reduced cost and unprecedented compactness. In recent years, there have been several critical experiments: the first demonstration of high-field (300 MV/m) speed-of-light electron acceleration in a fused silica structure [1], acceleration at sub-relativistic energies with an open grating [2], demonstration of a compatible optical-scale beam position monitor [3], high-gradient sub-relativistic acceleration at 220 MV/m [4] and at 370 MV/m [5] in silicon microstructures, and high-gradient (700 MV/m) acceleration of relativistic electrons using femtosecond laser pulses [6]. This approach has been colloquially referred to in the press as an “accelerator on a chip.” The high-gradient and wafer size of these accelerators make them very attractive for a future generation of high brilliance extreme ultraviolet (EUV) and X-ray sources. The DLA approach has the distinct features to produce attosecond electron bunches and can operate at 10s of MHz repetition rate. However, there are many accelerator science questions and technical challenges to address since the beam parameters for an accelerator based on this concept would be drastically different from both conventional accelerators and other advanced schemes.

The most powerful XUV and x-ray sources today are enabled by relativistic electron beams driven by state-of-the-art microwave linear accelerator facilities such as the Linac Coherent Light Source (LCLS) at SLAC. Recent research into novel dielectric laser accelerators (DLA) has given rise to the potential for new coherent radiative processes with attosecond pulses using dielectric structures with wavelength-scale periodic features excited by lasers at near-infrared wavelengths [1, 7], and with orders of magnitude higher accelerating fields than is possible with conventional microwave technology [6]. This approach has the potential to produce extremely bright electron beams in an ultra-

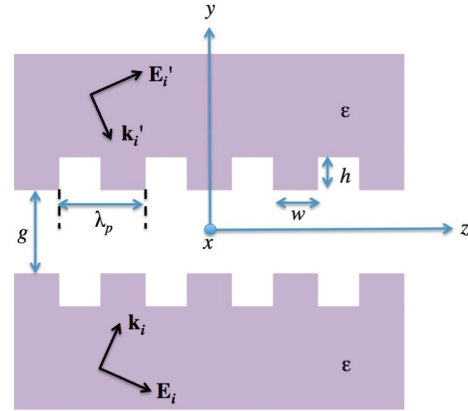


Figure 1: Planar symmetric geometry with periodic variation in  $z$ . Two exciting plane waves are shown incident from top and bottom.

compact footprint that are suitable for driving superradiant EUV light in a similarly optical-scale laser-induced undulator field. Radiation from each undulator/compressor module would add in amplitude but not in pulse length, maintaining the wide bandwidth and attosecond pulse structure. Preliminary calculations presented below suggest that a compact DLA driven by a  $2 \mu\text{m}$  infrared laser may generate a 10-fC, 200-as electron bunch train at 40 MeV particle energy. After passing 100 undulator/compressor modules, EUV radiation could be generated in a train of 660 as pulses separated by 6.6 fs laser period, with a pulse energy of more than 100 nJ. This attosecond pulse train would form an intense EUV frequency comb that would be extremely valuable for precision spectroscopy.

## LASER-DRIVEN DEFLECTION IN PLANAR STRUCTURE

All DLA structures experimentally tested to date have been of the planar symmetric variety (spatially invariant in one coordinate) and with a longitudinal periodicity along the particle beam axis. We here derive a generic form for the transverse forces in such a geometry which provide some helpful insights regarding development of a compatible laser-driven undulator. The wave equation for a linear material with spatially varying dielectric function  $\epsilon(\mathbf{r})$  may be written

$$\nabla^2 \mathbf{E} - \nabla(\nabla \cdot \mathbf{E}) = -(\omega/c)^2 \mathbf{D} \quad (1)$$

where  $\mathbf{D}$  is the electric displacement field, related to the electric field  $\mathbf{E}$  and polarization  $\mathbf{P}$  by  $\mathbf{D} = \mathbf{E} + 4\pi\mathbf{P}$ . We assume a dielectric, non-magnetic material ( $\mu = 1$ ), hence  $\mathbf{H} = \mathbf{B}$ . Solutions to Eq. 1 for given dielectric function

\* Work supported by U.S. Dept. of Energy, National Science Foundation, and Moore Foundation.

<sup>†</sup> england@slac.stanford.edu

# ATTOSECOND TIMING

F. X. Kärtner, M. Xin, and K. Safak

Center for Free-Electron Laser Science, Deutsches Elektronen-Synchrotron and  
 Physics Department and The Hamburg Center for Ultrafast Imaging, Universität Hamburg,  
 Hamburg, Germany

## Abstract

Photon-science facilities such as X-ray free-electron lasers (XFELs) and intense-laser facilities are emerging worldwide with some of them producing sub-fs X-ray pulses. These facilities are in need of a high-precision timing distribution system, which can synchronize various microwave and optical sub-sources across multi-km distances with attosecond precision. Here, we report on a synchronous laser-microwave network that permits attosecond precision across km-scale distances. This was achieved by developing new ultrafast timing metrology devices and carefully balancing the fiber nonlinearities and fundamental noise contributions in the system. New polarization-noise-suppressed balanced optical crosscorrelators and free-space-coupled balanced optical-microwave phase detectors for improved noise performance have been implemented. Residual second- and third-order dispersion in the fiber links are carefully compensated with additional dispersion-compensating fiber to suppress link-induced Gordon-Haus jitter and to minimize output pulse duration; the link power is stabilized to minimize the nonlinearity-induced jitter as well as to maximize the signal to noise ratio for locking.

Therefore, a multi-km attosecond-precision synchronization technique is imperative to unleash the full potential of these billion-dollar photon-science facilities.

The timing system consists of a reference providing extremely stable timing signals, a target signal that needs to be synchronized, a detector that can measure the timing difference between the target signal and the reference, and a control box to lock the timing of the target to that of the reference. If the target device is far away from the reference, a timing link is also necessary to deliver the timing signal from the reference to the target. Without exception, the attosecond-precision synchronization technique also requires these key elements.

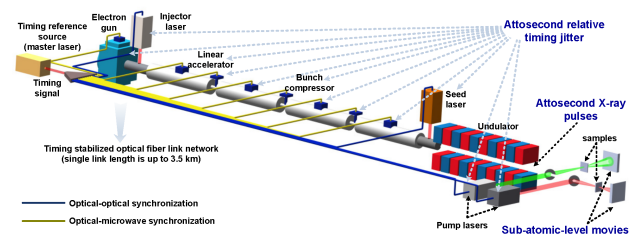


Figure 1: Timing and synchronization system for an attosecond XFEL [11].

## INTRODUCTION

Recently, several X-ray FELs (XFELs), such as the European XFEL [1] in Hamburg, FERMI [2] in Italy, SwissFEL in Switzerland and Linac Coherent Light Source (LCLS) [3] and LCLS II [4] in Stanford and Dalian Coherent Light Source (DCLS) and SXFEL in China have been built and are in operation. The length of these facilities ranges from few hundred meters to several kilometers. Many of these facilities aim to generate attosecond X-ray pulses [5] with unprecedented brightness to film physical and chemical reactions with sub-atomic-level spatio-temporal resolution [6, 7]. Significant progress in attosecond science, including the time-domain observation of intramolecular charge transfer [8] and the discovery of ultrafast Auger processes altering the chemistry of matter on an attosecond time scale [9, 10], has been made in the past few years. Thus current XFELs technology will move over the next decade into the attosecond regime. As illustrated in Fig. 1, it is advantages to generate attosecond X-ray pulses and perform attosecond-precision pump-probe experiments. This is supported in an optimum way, if all optical/microwave sources in the XFEL, including the electron gun, injector laser, microwave references of the linear accelerator and bunch compressor, most importantly, the seed laser and pump lasers at the end station are synchronized simultaneously with attosecond relative timing jitter.

The timing reference source in attosecond synchronization can be an atomic clock [12, 13], a continuous-wave (CW) laser [14, 15] or a mode-locked laser [16, 17]. The state-of-the-art technique in each solution can provide an attosecond-jitter-equivalent instability for 1s observation time. In contrast to the other two solutions, a mode-locked laser can simultaneously provide ultralow-noise optical and microwave signals, and the ultrashort optical pulses in time domain can be directly used as time markers for precise timing measurements. So it is an ideal timing source for synchronization applications such as telescope arrays and XFELs, where the target devices are mode-locked lasers and microwave sources.

Another advantage of using mode-locked lasers is that it can provide very high sensitivity during timing detection, thanks to its high pulse peak power. For example, we have developed balanced optical cross-correlators (BOCs) [17, 18] and balanced optical-microwave phase detectors (BOMPDS) [19–21] for optical-optical and optical-microwave timing detection, respectively. Both of them can achieve attosecond precision and >1-ps dynamic range at the same time.

For remote synchronization, the timing link can be implemented as optical fiber link [22]. Optical-fiber-based timing

## COMPACTLIGHT DESIGN STUDY\*

- A. Latina<sup>†</sup>, D. Schulte, W. Wuensch, S. Stapnes, CERN, 1211 Geneva 23, Switzerland  
G. D’Auria, R. Rochow, Elettra Sincrotrone Trieste, 34149 Basovizza, Italy  
J. Clarke, STFC Daresbury Laboratory, Warrington, WA4 4AD, UK  
W. Fang, Shanghai Institute of Applied Physics, Shanghai 201800, P. R. China  
E. Gazis, Institute of Accelerating Systems and Applications, IASA, Athens, Greece  
M. Jacewicz, Uppsala Universitet, UU, Uppsala, Sweden  
R. Dowd, ANSTO, Lucas Heights, NSW 2234, Australia  
A. Aksoy, Ankara University Institute of Accelerator Technologies, UA-IAT, Ankara, Turkey  
H. Prien, VDL Enabling Technology Group, VDL ETG, Eindhoven, Netherlands  
M. Ferrario, Istituto Nazionale di Fisica Nucleare, LNF-INFN, Frascati, Italy  
R. Geometrante, Kyma S.r.l., Trieste, Italy  
A. Mostacci, University of Rome “La Sapienza”, Rome, Italy  
F. Nguyen, ENEA, Roma, Italy  
F. Perez, ALBA Synchrotron, 08290 Cerdanyola de Vallès, Barcelona, Spain  
A. Faus-Golfe, Centre National de la Recherche Scientifique, CNRS, Paris, France  
A. Bernhard, Karlsruher Institut für Technologie, KIT, Karlsruhe, Germany  
T. Schmidt, Paul Scherrer Institut, 5232 Villigen PSI, Switzerland  
D. Esperante, Agencia Estatal Consejo Superior de Investigaciones Científicas, CSIC, Madrid, Spain  
M. Aicheler, University of Helsinki, UH/HIP, Helsinki, Finland  
A. Cross, University of Strathclyde, USTR, UK

### Abstract

H2020 CompactLight Project aims at designing the next generation of compact hard X-Rays Free-Electron Lasers, relying on very high accelerating gradients and on novel undulator concepts. CompactLight intends to design a compact Hard X-ray FEL facility based on very high-gradient acceleration in the X band of frequencies, on a very bright photo injector, and on short-period/superconductive undulators to enable smaller electron beam energy. If compared to existing facilities, the proposed facility will benefit from a lower electron beam energy, due to the enhanced undulators performance, be significantly more compact, as a consequence both of the lower energy and of the high-gradient X-band structures, have lower electrical power demand and a smaller footprint. CompactLight is a consortium of 24 institutes (21 European + 3 extra Europeans), gathering the world-leading experts both in the domains of X-band acceleration and undulator design.

### MOTIVATION AND OBJECTIVES

Our aim is to facilitate the widespread development of X-ray FEL facilities across Europe and beyond, by making them more affordable to construct and operate through an optimum combination of emerging and innovative accelerator technologies. We will design a Hard X-ray FEL facility using the very latest concepts for bright electron photo injectors,

very high-gradient accelerating structures and novel short period undulators. The resulting facility will benefit from a lower electron beam energy than current facilities, due to the enhanced undulator performance, will be significantly more compact as a consequence of this lower energy as well as due to the application of very high-gradient structures, and also have a much lower electrical power consumption than current facilities through the use of an X-band RF system at 12 GHz. These ambitious but realistic aims will result in much lower construction and running costs making X-ray FELs affordable, even by national institutions or academia. We therefore anticipate that our Design Study will enable FEL facilities to proliferate across all of Europe and beyond much more rapidly than third generation light sources have managed over the past decades.

CompactLight gathers the world-leading experts in these domains, united to achieve two objectives: disseminate X-band technology as a new standard for accelerator-based facilities and advance undulators to the next generation of compact photon sources, with the aim of facilitating the widespread development of X-ray FEL facilities across and beyond Europe by making them more affordable to build and to operate.

### A COMPACT HARD X-RAY FEL

A standard layout of an FEL is shown in Fig. 1. It consists of a high-brightness electron source, a pre-acceleration section up to about 300 MeV, a laser heater, to optimize the micro-bunching instability, three linear accelerating sections (L1, L2, and L3 in the figure), and two magnetic chicanes,

\* This project receives funding from the European Union’s Horizon 2020 research and innovation programme topic Design Studies.

<sup>†</sup> andrea.latina@cern.ch

# QUAPEVA: VARIABLE HIGH GRADIENT PERMANENT MAGNET QUADRUPOLE

C. Kitegi, T. André, F. Blache, M.E. Couprie, A. Ghaith, J. Idam, A. Loulergue, F. Marteau, D. Oumbarek, M. Sebdaoui, M. Valléau, J. Vétéran, SOLEIL, Gif-sur-Yvette, France  
 C. Benabderrahmane, J. Chavanne, G. Le Bec, ESRF, Grenoble, France  
 O. Cosson, F. Forest, P. Jivkov, J. L. Lancelot, Sigmaphi, Vannes, France  
 C. Vallerand, LAL, Orsay, France  
 P. N’gotta, MAX IV, Lund, Sweden

## Abstract

The magnetic and the mechanical design of a high and variable gradient Permanent Magnet Quadrupole (PMQ) is presented. Seven of them with various lengths, ranging from 26 mm up to 100 mm, for different integrated quadrupole strengths were manufactured. The measured magnetic performance of these devices is also reported. These devices were successfully commissioned to transport laser plasma accelerated electron beam.

## INTRODUCTION

Current accelerator projects require strong quadrupole magnets to focus particle beams to ever smaller size. They rely on the very mature resistive magnet technology for gradient below typically 100 T/m. For larger gradient, Permanent Magnet (PM) technology seems to be attractive alternative as the highest gradient value ever reported with a PMQ is 575 T/m for a 2.75 mm bore radius [1]. However, since the first proposal of PM multipole design in the early eighties [2], their use in accelerators stayed marginal. Their relative poor field quality and the small field tuning has limited them to specific applications such as final focus system in colliders [3-5] or in projects where PM technology offers a clear and substantial saving over resistive technology [6].

A fixed gradient quadrupole targeting standard field quality of light source accelerator magnet, which smears the difference between the magnetic performance obtained with resistive and PM accelerator magnets, was recently developed at the ESRF [7].

We present hereafter the design of the QUAPEVA, a variable high gradient PMQ, i.e. with a gradient larger than 100 T/m and 50 % tunability [8-11]. As far as the amplitude of the gradient adjustment is concerned, this design also brings PM accelerator magnet closer to resistive magnet. One prototype and two triplets were manufactured for an experiment dedicated to the demonstration of a COherent X-ray source INferred from Electrons accelerated by Laser (COXINEL) [12]. We first introduce the concept and the parameters for QUAPEVA COXINEL, we then present the magnetic performance of the seven built items.

## QUAPEVA CONCEPT

### General Description

The magnetic design of QUAPEVA is shown in Fig. 1. The magnet structure is made of two concentric quadrupoles. The inner quadrupole follows the Halbach hybrid arrangement of PM and soft iron poles to drive the PM magnetic flux into the gap. The soft iron poles also smooth the PM magnetic imperfections and thus help improving the field quality. The outer quadrupole is dedicated to the field gradient tuning and is composed with a set of four cylindrical PM magnetized in radial direction. Each magnet is located at the top of one of the inner quadrupole soft iron pole. The soft iron shield placed behind each rotatable magnet limits the field leakage from the outer quadrupole.

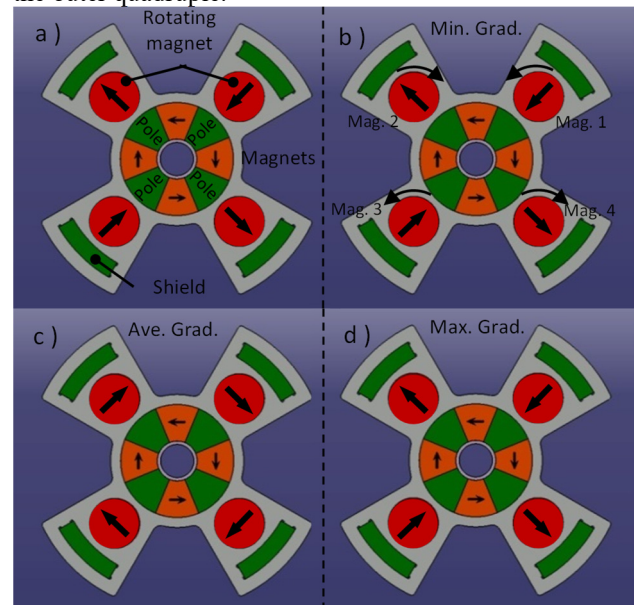


Figure 1: Schematic of the QUAPEVA magnetic design (a). Orientation of the four rotating magnets at minimum gradient (b), average gradient (c) and maximum gradient (d).

## ANALYSIS OF ELECTRON TRAJECTORIES IN HARMONIC UNDULATOR WITH SCILAB'S MODEL BASED DESIGN CODES

H. Jeevakhan, S. Kumar, National Institute of Technical Teachers' Training and Research,  
 Bhopal, India

G. Mishra, Physics Department, Devi Ahilya University, Indore, India

### Abstract

Scilab's X-cos model-based simulation blocks have been used to simulate the trajectories of an electron traversing through a Harmonic undulator. The **trajectory** of electron along X direction has been simulated from Numerical and analytical methods. Analysis given in the present paper is compared with the other codes. Parallel simulation of Harmonic undulator magnetic field along with trajectories of electron is given in the present analysis.

### INTRODUCTION

Fourth generation X-Ray Free electron laser (XFEL) light source is the state of art technology and have number of applications in cutting edge multidisciplinary research areas [1]. Spectral properties of out coming radiation in FEL depend upon numbers of parameters such as beam quality, magnetic structure, seed laser, trajectory of electron traversing in undulator and many more. Simulation software such as Radia and Poison are often used to design Undulator and calculate the magnetic field at on and Off axis. The raw data of magnetic field profile obtained from the simulation or measurements by Hall Probe method can be analysed to determine electron trajectories, intensity of spontaneous radiation, FEL gain in stimulated emission.

Model-based development (MBD) is a paradigm shift in software development. It's mainly focuses on executable models of the systems of equations. These models allow a wide range of analysis. Compare to traditional design flow, model-based design condensed development time. The main factors that contributed to the substantial reduction in development time is achieved by using model-based design: clocking, defect discovery, and component interfaces [2].

Scilab/Xcos an open source technology [3] had been used for number of applications such as remote control lab, real time experiments, and CDMA modelling [4-6]. Scilab/Xcos based simulation models for analytical solutions of electron trajectory equations have been presented with some limitations by H Jeevakhan etal [7]. In present analysis X-cos based on model based design has been employed to find the trajectory of the electron moving in the Harmonic undulator, variation of magnetic field along the axis of undulator. We have also presented a model to analyze trajectory in the magnetic field profile given by real undulator measurements and simulated by RADIA software.

### PRESENT SIMULATION-UNDULATOR FIELD

Planar undulator magnetic field with additional small harmonic field is considered for simulation and is given by [8-9]

$$B = [0, a_0 B_0 (\sin k_u z + \Delta \sin k_h z), 0] \quad (1)$$

Where,  $k_u = \frac{2\pi}{\lambda_u}$  and  $k_h = \frac{2\pi}{\lambda_h}$  where  $k_u$  and  $k_h$  are undulator and harmonic undulator wave number respectively,  $\lambda_u$  is undulator wave length and  $\lambda_h = h\lambda_u$ ,  $h$  is harmonic integer,  $B_0$  is peak magnetic field,  $\Delta = \frac{a_1}{a_0}$ ,  $a_0$  and  $a_1$  controls the amplitude of main undulator field and additional harmonic field respectively

The velocity and trajectory of electron in 'x' direction are deduced by using Lorentz force equation reads as

$$\beta_x = -\frac{K}{\gamma} \left[ \cos(\Omega_u t) + \Delta \frac{\cos(h\Omega_u t)}{h} \right] \quad (2)$$

$$\frac{x}{c} = -\frac{K}{\gamma} \left[ \frac{\sin(\Omega_u t)}{\Omega_u} + \Delta \frac{\sin(h\Omega_u t)}{h\Omega_u} \right] \quad (3)$$

Where  $\gamma$  is relativistic parameter,  $K = \frac{a_0 e B_0}{\Omega_u m_0 c}$  is the undulator parameter,  $m_0$  is rest mass of electron, and  $\Omega_u = k_u c$

### SIMULATION PARAMETERS

Analytical solution of trajectory along 'x' direction is simulated with the magnetic field given in Eq.(3) and Eq.(1) respectively. Table 1 gives the parameters of simulation used in the analysis. SCILAB's Model based simulation model using Xcos tool boxes has been designed for Eq.(3) and Eq.(1). Each parameter in Table 1 is identified by a block in the simulation model. The parameter values can be changed by selecting the relevant block and alteration can be done.

Table 1: Parameters used for Simulation

Parameter	Symbol	Values
Undulator parameter	K	1
Number of Undulator periods	N	10
Undulator wavelength	$\lambda$	5cm
Relativistic parameter	$\gamma$	20
Harmonic integer	h	3
Contribution of harmonic field	$\Delta$	0, 0.1, 0.2, 0.4

# HARMONIC UNDULATOR RADIATION WITH DUAL NON PERIODIC MAGNETIC COMPONENTS

H. Jeevakhan, National Institute of Technical Teachers' Training and Research, Bhopal, India  
G. Mishra, Physics Department, Devi Ahilya University, Indore, India

## Abstract

Undulator radiation at third harmonics generated by harmonic undulator in the presence dual non periodic constant magnetic field has been analyzed. Electron trajectories along the 'x' and 'y' direction has been determined analytical and numerical methods. Generalized Bessel function is used to determine the intensity of radiation and Simpson's numerical method of integration is used to find the effect of constant magnetic fields. Comparison with previous analysis has also been presented.

## INTRODUCTION

Free electron Lasers (FEL) generation is a state of art technology and has large numbers of applications in cutting edge technologies [1]. Tunability and brilliance at lasing wave length in FEL are the key parameters for number of research applications. Lasing wavelength of FEL depends upon the values of undulator parameter, undulator wavelength and relativistic parameter of electron beam. Recent works in FEL theory has emphasised the effect on non periodic magnetic field i.e. constant magnetic field component along or perpendicular or in both directions of the periodic magnetic field of planar undulator on the out coming undulator radiation(UR)[2-3]. Partial compensation on the divergence of UR has been demonstrated by imposing weak constant magnetic component in the analytical form and all the major sources of homogeneous and inhomogeneous broadening have been accounted for the characteristics of the electrons beam by K. Zhukovsky [4]. The constant non-periodic magnetic constituents are studied to compensate the divergence of the electronic beam [5]. Dattoli *et al* has initially reported the effect on UR from planar undulator with constant magnetic field component [6]. The later studies focuses on higher harmonics generation by addition of additional harmonic field [2-5].

Higher harmonic generation has been studied by using Harmonic undulator (HU) consists additional harmonic field along with sinusoidal planar magnetic field[7-13]. HU uses modest electron beam energy and lasing at third harmonic is reported by N.Sei *et al* [14]. The harmonic field can be generated by the addition of shims in the planar undulator structure[15-17]. Constant magnetic field may present due to errors in Undulator design and horizontal component of earth's magnetic field and modify the UR Magnetic field. H Jeevakhan *et al* have presented semi analytical results for the effect of perpendicular constant magnetic field on the gain of HU at higher harmonics [3,18]. In the present paper we have analysed HU with dual non periodic magnetic field. In the previous

reported works the independent effect of constant magnetic field, parallel and perpendicular to planar undulator field had been analysed. The combined effect on intensity reduction due dual magnetic field has been presented. The additional harmonic field compensates the intensity loss in UR in presented model.

## UNDULATOR FIELD

Planar undulator sinusoidal magnetic field encompasses with a perpendicular constant magnetic field in present analysis and is given by

$$B = [B_0\kappa_x, a_0B_0(\sin k_u z + \Delta \sin k_h z) + B_0\kappa_y, 0] \quad (1)$$

Where,  $k_u = \frac{2\pi}{\lambda_u}$  and  $k_h = \frac{2\pi}{\lambda_h}$  where  $k_u$  and  $k_h$  are undulator and HU wave number respectively,  $\lambda_u$  is undulator wave length and  $\lambda_h = h\lambda_u$ ,  $h$  is harmonic integer,  $B_0$  is peak magnetic field,  $\Delta = \frac{a_1}{a_0}$ ,  $a_0$  and  $a_1$  controls the amplitude of main undulator field and additional harmonic field,  $\kappa_y$  and  $\kappa_x$  are the magnitudes of constant non periodic magnetic field parallel and perpendicular to main undulator field.

The velocity of electron passing through undulator is derived by using Lorentz force equation:

$$\frac{dv}{dt} = -\frac{e}{\gamma mc} (\vec{v} \times \vec{B}) \quad (2)$$

This gives

$$\beta_x = -\frac{K}{\gamma} \left[ \cos(\Omega_u t) + \Delta \frac{\cos(h\Omega_u t)}{h} - \kappa_y \Omega_u t \right] \\ \beta_y = -\frac{K}{\gamma} \kappa_x \Omega_u t \quad (3)$$

$$\beta_z = \beta^* - \frac{K^2}{2\gamma^2} \left[ \left\{ \frac{1}{2} \cos(2\Omega_u t) + \frac{1}{2} \left( \frac{\Delta}{h} \right)^2 \cos(2h\Omega_p t) + \left( \frac{\Delta}{h} \right) \cos(1 \pm h)\Omega_u t - 2\kappa_y \Omega_u t \cos(\Omega_u t) - 2\kappa_y \Omega_u t \cos(h\Omega_u t) \right\} + (\kappa_x^2 + \kappa_y^2) \Omega_u^2 t^2 \right] \quad (4)$$

Where  $m$  and  $m_0$  are relativistic and rest mass of electron respectively and value of  $m$  is governed by the relativistic parameter  $\gamma$ ,  $K = \frac{a_0 e B_0}{\Omega_u m_0 c}$  is the undulator parameter and

$$\beta^* = 1 - \frac{1}{2\gamma^2} \left[ 1 + \frac{K^2 + K_1^2}{2} \right] \text{ with } K_1 = \frac{\Delta K}{h} \text{ and } \Omega_u = k_u c.$$

The solution of Eq. 4 gives the electron trajectory along z direction,

# UNDULATOR PHASE MATCHING FOR THE THE EUROPEAN XFEL

Y. Li, J. Pflueger, European XFEL GmbH, Hamburg, Germany

## Abstract

The undulator system in the European XFEL is mainly comprised 5-m long undulator segments and 1.1 m long intersections in between. In intersections the electron velocity is faster than it inside an undulator and the optical phase is detuned. The detune effect is also from the undulator fringe field where electron longitudinal speed also deviates from the oscillation condition. The total detune effect is compensated by a magnetic device called phase shifter, which is correspondingly set for a specific undulator gap. In this paper we introduce the method to set the phase shifter gap for each K parameter according to the measured magnetic field.

## INTRODUCTION

High gain free electron lasers (FELs) using the principle of Self-Amplified Spontaneous Emission (SASE) are so far the only way to generate FEL radiation in the hard X-ray range [1-5]. For VUV radiation alternatives such as harmonic generation exist generate radiation which lead to increased stability [6]. However, aside from such differences both require long undulator systems with lengths from tens of meters up to about 200 meters depending on the radiation wavelength, electron beam and undulator parameters. Such a long undulator system cannot be built as a continuous device. For practical reasons of manufacturing it must be segmented into lengths around typically 5m maximum.

For the FEL process the interruption of the undulator implies a problem: The longitudinal speed of the electrons in the intersection is different to that inside the undulator and therefore the optical phase matching between laser field and electron motion is perturbed. In a fixed gap undulator system such as FLASH [1,2] or LCLS I [3] phase matching can be obtained by choosing the intersection length and tuning the end fields of the undulator segments properly. The phase matching in a gap tunable system is more complicated since the phase mismatch in the intersection changes with undulator gap. With a phase shifter, a small magnetic chicane, an additional delay is induced in the electron orbit. By properly selecting the phase shifter strength and hence the delay the optical phase can be matched at any gap [7].

The European X-ray free electron laser (EXFEL) facility [5] is a large project driven by a 1.8 kilometer long superconducting linac. The SASE FEL is used throughout the European XFEL. An electrons beam is accelerated up to maximum of 17.5 GeV. Then it is guided through the undulator system to generate high quality soft and hard X-rays. The radiation wavelength can be changed by variation of the undulator gap and in addition the beam energy: The hard X-ray range from 0.1 to 0.4 nm is covered by two undulator lines called SASE1 and SASE2. The soft X-Ray wavelength range from 0.4 to 1.6 nm is covered by one undulator line called SASE3.

For all SASE beam lines the undulators and phase shifters are well characterized before installation: Undulators were accurately tuned for small trajectory and phase errors in the operational gap range [8,9]. After tuning the characterization for each segment includes high resolution field maps as a function of gap in 0.5mm steps. They are the basis for the calculation of device properties such as K-Parameter, optical phase errors, trajectory wander etc. All phase shifters were well tuned and characterized as well [10-13].

An undulator system comprised of many segments is best controlled by the K-Parameter, which directly relates to the radiation wavelength, and not by the individual gaps, which differ slightly from segment to segment due to manufacturing and material tolerances. The K-parameter plays a key role and needs to be provided with an accuracy of  $\Delta K/K \leq 2 \times 10^{-4}$ .

## PHASE MATCHING STRATEGY

### Practical Situation

One feature of the undulator system for SASE FEL is that all segments must work cooperatively: In order not to deteriorate the FEL process the individual K-parameters need to be provided with an accuracy determined by  $\Delta K/K \leq \rho$  where  $\rho$  is the Pierce parameter, which for EXFEL is about  $2 \times 10^{-4}$ . Therefore in an undulator system the gaps of individual undulator segments need to be adjusted so all match the same K.

On the other side field measurement on undulators is made by controlling the gap, which can be directly controlled mechanically with micrometer precision. Therefore, the K-parameters for each segment needs to be evaluated by interpolation from measurements made at different gaps.

### Phase Matching Criteria

Figure 1 illustrates two undulator cells. Each cell is subdivided into four regions: On going from left to right the beginning of a cell is chosen in the field free region in the very left before the undulator. The region from at the beginning of the cell to the beginning of undulator bulk poles, including the drift space and the undulator fringe field, is called entrance fringe. The phase advance in this part is  $\varphi_{\text{Entr}}$ . The periodic field region inside the undulator is called bulk field. The phase advance over this region is  $\varphi_{\text{Bulk}}$ . Ideally at the first harmonic the phase advance in this region is  $2\pi$  per period. Similar to the entrance fringe the region from the end of bulk field to the beginning of phase shifter is called exit fringe with the phase advance  $\varphi_{\text{Exit}}$ . In the field free region after the exit fringe the phase shifter is placed. The phase advance over the phase shifter is  $\varphi_{\text{PS}}$ . Since the phase shifter has very low fringe fields [7], it does not interfere with the undula-

# MICROBUNCHING INSTABILITY STUDY IN THE LINAC-DRIVEN FERMIL FEL SPREADER BEAM LINE\*

S. Di Mitri<sup>†</sup>, S. Spampinati, Elettra – Sincrotrone Trieste S. C. p. A., Basovizza, Trieste, Italy

## Abstract

Suppression of microbunching instability (MBI) along high brightness electron beam delivery systems is a priority for Free Electron lasers (FELs) aiming at very narrow bandwidth. The impact of MBI on FEL spectral brilliance is aggravated by the growing demand for multi-user FEL facilities, which adopt multi-bend switchyard lines traversed by high charge density electron beams. This study provides practical guidelines to switchyards design largely immune to MBI, by focusing on the FERMI FEL Spreader line. First, two MBI analytical models [Z. Huang and K.-J. Kim, Phys. Rev. Special Topics - Accel. Beams 5, 074401 (2002); R.A. Bosch, K.J. Kleman and J. Wu, Phys. Rev. Special Topics - Accel. Beams 11, 090702 (2008)] are successfully benchmarked along the accelerator. Being the second model flexible enough to describe an arbitrary multi-bend line, and found it in agreement with particle tracking and experimental results, it was used to demonstrate that a newly proposed Spreader optics provides unitary MBI gain while preserving the electron beam brightness.

## INTRODUCTION

In FEL facilities with multiple undulator lines, the strength of the microbunching instability (MBI) is reinforced in multi-bend switchyard lines that connect the accelerator to the individual undulator lines [1–5]. Due to the presence of several dipole magnets traversed by a high charge density beam, those switchyards can dramatically amplify residual density and energy modulations present on the electron beam at the exit of the linac. This study examines MBI growth in the accelerator and switchyard, and provides practical guidelines for switchyard optics designs that are largely immune to MBI, i.e., with unity gain of the instability. We provide a specific solution for the FERMI FEL [6,7] spreader beam line that can be easily implemented within the current space and with existing magnets [8].

MBI in the FERMI linac has been continuously studied since the early stages of machine design [9–11]. MBI concerns led to the choice of operating FERMI both with a so-called laser heater (LH) [12,13], a tool that suppresses MBI via energy Landau damping, and in general using only one active magnetic bunch length compressor [9]. The FERMI laser heater usually improves the FEL spectral brilliance by up to factors 3 or more [13,14]. Nonetheless, there is experimental evidence [11,15] of both enlargement and shot-to-shot variability of the spectral bandwidth for wavelengths 10 nm or shorter. Provisionally, this degradation is assigned to effects originating with residual MBI from the linac and to its further amplification in the spreader.

This paper aims to elucidate the role of the FERMI spreader on the MBI development.

## MODELS

The reader is sent to [16] the MBI model developed by Z. Huang and K.-J. Kim (henceforth labeled the “HK-model”), and based on integral equations for the bunching factor, i.e., the Fourier transform of the bunch current density function. The reader is sent to [17] for the MBI model developed by R. Bosch et al. (henceforth labeled the “B-model”), and based on matrix formalism. All collective effects are described by frequency-dependent effective impedances separately calculated for linac straight sections and chicane dipole bend sections.

The HK- and the B-models have been compared by adopting a shot-noise driven initial density modulation that has no corresponding energy modulation. The initial bunching factor is taken to be:

$$b_{sn}(\lambda_0) = \sqrt{\frac{2ec}{I_0\lambda_0}} \quad (1)$$

An additional indicator of the MBI strength, used for the comparison of the two models, is given by the amount of energy spread accumulated by the end of the beam line. Assuming that the final energy modulations are entirely converted into uncorrelated energy spread, the equivalent uncorrelated energy spread (RMS value) from the MBI growth is calculated as the integral of the final energy modulation over all (or user-specified) frequency components [18]:

$$\sigma_{E,MBI} = \frac{1}{2\pi\sqrt{2}} \sqrt{\int d\lambda \frac{\Delta E_{MBI}^2(\lambda)}{\lambda}} \quad (2)$$

The HK- and the B-model both include originally Coherent Synchrotron Radiation (CSR) and Longitudinal Space Charge (LSC) impedance, energy- and transverse emittance-induced Landau damping. They were further revised for the purpose of comparison as follows:

- i) the LSC impedance is averaged over the transverse beam dimensions, which vary along the linac, according to the prescriptions in [19,20];
- ii) the MBI gain is evaluated by keeping the initial bunching factor, i.e., the low gain regime is retained together with the high gain contribution [13];
- iii) the effect of the LH on the electron beam initial energy distribution was calculated as in [21], assuming a laser pulse whose transverse waist size is matched at the midpoint of the LH undulator to that of the electron beam;
- iv) for a fair comparison of the two models, the B-model was applied to the FERMI linac by excluding the im-

## STRONG FOCUSING LATTICE DESIGN FOR SSMB

Tenghui Rui<sup>†</sup>, Xiujie Deng, Alex Chao<sup>1</sup>, Wenhui Huang, Chuanxiang Tang,  
 Tsinghua University, Beijing, China  
<sup>1</sup> also at SLAC, Menlo Park, USA

### Abstract

A storage ring applicable for SSMB operation is a critical part of a high average power SSMB EUV light source. A lattice for SSMB based on longitudinal strong focusing is under design in Tsinghua University. To generate and maintain micro-bunching in a storage ring in this scenario, the momentum compaction has to be small. A lattice with low momentum compaction factor is presented in this work. The lattice of the current design consists of two MBA cells with isochronous unit cells to

To develop microchips with etched circuit lines smaller than 0.1um, new technology is needed. Extreme ultraviolet lithography is a next generation of lithography technology and the wavelength is expected to be 13.5nm, while DUV's wavelength is 193nm or 248nm. A microprocessor made with the EUVL technology would be a hundred times more powerful than today's. SSMB (Steady State Micro-Bunching) is a promising scheme for high average power EUV light sources.

When electrons are grouped into micro bunches spaced at the wavelength of desired radiated light, the radiation process is coherent and the brightness of the resulting light is orders of magnitude higher than that of an equivalent incoherent light source. In a linac based light source such as conventional FELs, the electron bunch passes through the radiator once, leading to low duty cycles, and thus the average radiation power is limited. In the contrast, storage rings offer a much higher repetition rate and potentially produce much higher average radiation power. In this work, our attempts at designing a storage ring applicable for SSMB operation are presented.

### LOW MOMENTUM COMPACTION LATTICE

Based on conventional formulas, the bunch length in a storage ring is related to momentum compaction factor and RF parameters.

$$\sigma_z = \frac{\eta \sigma_\delta c}{2\pi \nu_s} = \frac{(\alpha_c - 1/\gamma^2) \sigma_\delta c}{2\pi \nu_s}, \quad (1)$$

where  $\alpha_c$  is the momentum compaction factor,  $\gamma$  is the Lorentz factor, and  $\nu_s$  is the synchrotron tune. Synchrotron tune depends on RF parameters and momentum compaction factor [4]:

minimize local and global momentum compaction, and two straight sections for insertion devices. The design energy of the ring is 400MeV and the circumference is 94 meters. Nonlinear effects such as higher order momentum compactions will continue to be optimized.

### INTRODUCTION

Deep ultraviolet lithography, which is the current technology used to produce microchip, begins to reach its limit

$$\nu_s = \sqrt{\frac{h e V |\eta \cos \phi_s|}{2\pi \beta^2 E}}, \quad (2)$$

where  $h$  is the harmonic number,  $V$  is the RF voltage and  $\phi_s$  is the synchronous phase. According to these formulas, equilibrium bunch length is proportional to the square root of slip factor, and by reducing momentum compaction, the bunch length can be shortened to realize sustained micro bunching.

Momentum compaction factor is directly defined as the integral of the dispersion function.

$$\alpha_c = \frac{1}{c} \int \frac{\eta_x}{\rho} ds. \quad (3)$$

To achieve low momentum compaction, the most straightforward way to do is to make the dispersion in bending magnets cancel out. Figure 1 shows a conventional double bend achromat. The strengths of the quadrupole magnets between the two dipole magnets are chosen such that the dispersion function is symmetric about the central quadrupole. To achieve low momentum compaction, the strength of the central quadrupole can be tuned to introduce asymmetry into the dispersion function. As is shown in Fig.2, the dispersion function in the two bending magnets is opposite in sign. As a result, the compaction factor can be small.

Figure 3 shows the layout of the first version of the SSMB lattice. The calculation of the beta function is done with Elegant.[1] The lattice consists of four cells. Each cell consists of two dipole magnets with cancelling dispersion function. Each pair of the cells has symmetrical optical functions so two cells form a four bend achromat with the straight sections on both ends free of dispersion. The dispersion free sections can accommodate equipment like RF cavity or undulator.

<sup>†</sup> email address: rth13@mails.tsinghua.edu.cn

# THE DESIGN AND TEST OF A STRIPLINE KICKER FOR HEPS

H. Shi, J. H. Chen, L. Wang, N. Wang, L. H. Huo, P. Liu, G. W. Wang, X. L. Shi,  
 Key Laboratory of Particle Acceleration Physics and Technology, Institute of High Energy Physics,  
 Chinese Academy of Sciences, Beijing 100049, China

## Abstract

A fast stripline kicker is adopted for High Energy Photon Source (HEPS) on-axis injection. The optimization of a prototype 750 mm long kicker has been finished. The 3D simulation results show the final design of wide vane with end cover lowers the beam loss about 31% than the original design does. We develop a feedthrough model with machinable glass ceramic and achieve a VSWR under 1.3 in 0~2 GHz. The assembly of kicker and commercial feedthroughs has been tested with Keysight E5071C. The testing results of S parameters and TDR value show a good agreement with simulation ones.

Table 1: Specifications of the Stripline Kicker for HEPS-TF

Parameters	Value
Length of blades (mm)	750
Gap between the two blades (mm)	10
Good field region (mm)	$\pm 2.3$ (x) $\pm 1.0$ (y)
Field uniformity	2%
Odd-mode impedance ( $\Omega$ )	$50 \pm 0.5$
Even-mode impedance ( $\Omega$ )	$60 \pm 0.5$
Operation pulse voltage (kV)	$\pm 20$
Degree of vacuum (Torr)	$1 \times 10^{-9}$

## INTRODUCTION

High Energy Photon Source (HEPS) is a storage ring light source with the beam energy of 6 GeV. The effective dynamic aperture (DA) is about 2.5 mm (horizontal) and 3.5 mm (vertical), which is not large enough for off-axis injection [1]. On-axis swap-out injection or on-axis longitudinal accumulating injection schemes are proposed, and a very fast kicker is required for both on-axis injection systems [2].

In the HEPS test facility (HEPS-TF) project, a stripline kicker of 750 mm long has been designed and tested as one of key hardware techniques. Figure 1 gives the section view of the stripline kicker and high voltage feedthroughs. The design has been optimized to satisfy the specifications of the kicker, such as the matching odd-mode impedance, field uniformity in good field region, and minimizing the local electric field in operation voltage, which are shown in Table 1 [3].

In this paper, we'll first give the detailed optimization of kicker with 3D simulation. Then the preliminary design of feedthrough is presented. Finally, we'll compare the simulation and testing results of the prototype kicker.

## KICKER DESIGN OPTIMIZATION

The two-blade stripline kickers have been successfully operating at KEK [4] and DAΦNE [5]. New designs have been developed to achieve high field uniformity, maximum kicker strength, low beam impedance and short pulse width [6-8].

Our kicker design refers to the APS-U design [8-10] because of the similar machine parameters. Figure 2 shows the basic geometry of the kicker body. Robust "D" shape blades are adopted for easily achieving high field homogeneity, where  $a$ ,  $b$  are the axes of the central ellipse,  $blade$  is the thickness,  $gap$  is the half distance, which define the blades geometry. The outer body half shell is composed of 2 connected half ellipses, where  $X_c$ ,  $a_0$ ,  $b_0$  defines the central half ellipse, and  $X_c$ ,  $a_{00}$ ,  $b_0$  defines the outer half ellipse. Adjusting the  $vane$  value can improve the mismatching of the even-mode impedance.

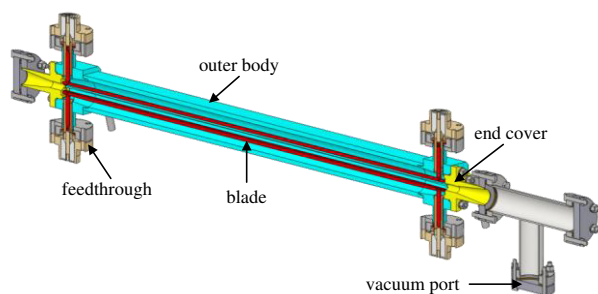


Figure 1: Section view of the stripline kicker.

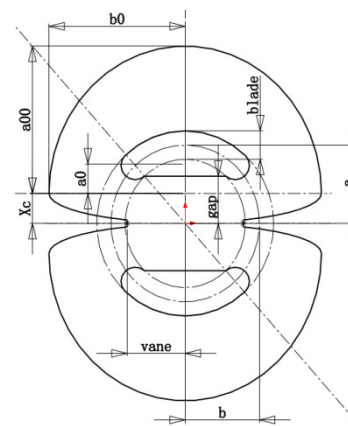


Figure 2: Basic geometry of the cross section.

The whole kicker consists of the main part of 650 mm and two taper parts of 50 mm, as shown in Figure 3. The odd-mode and even-mode impedance are optimized at the section of main part and end section of taper part

# PHASE SHIFTER APPLICATION IN DOUBLE UNDULATOR CONFIGURATION OF HEPS

X. Y. Li, Y Jiao, S.K Tian

Key Laboratory of Particle Acceleration Physics and Technology, Institute of High Energy Physics, 100049 Beijing, China

## Abstract

For over 6 meters long straight-section of HEPS, collinear double-cryogenic permanent magnet undulator(CPMU) is designed for high energy photon users to achieve higher brightness. Angular and spatial profiles of radiation produced by the double undulator configuration have been derived analytically. The efficiency of phase shifter on improving the brightness of double-CPMU is therefore evaluated with the beam energy spread and emittance are taken into account. Optimized beta-functions of electron beam are obtained.

## INTRODUCTION

In the first phase of HEPS construction, a total of 14 ID-based beamlines are required for constructed, of which 7 are based on in-vacuum undulators [1]. In order to satisfy the requirement of high-energy users, the phase error of these Ids should be reduced to below 2-3 ° especially for the application of harmonics higher than 9th. Therefore, the maximum length of in-vacuum undulator has to be less than 3 meters due to the limitations of the current manufacturing process. This leads to the necessity of installing two undulators in series on one 6 meters long straight section. In this case, if it is necessary to install an additional phase shifter between the two undulators and its effects on the radiation performance when considering the real beam parameters has become a significant problem should be investigated.

An intuitive view of this issue is that it does necessary for the phase matching between the two undulators. coherence effect will increase the on-axis radiation intensity to 4 times higher that of single undulator for maximum which equivalent to an undulator with the total length doubled or reduce it to zero for minimum in the case of phase mismatch. The effects of emittance and energy spread has been ignored yet which cause this view divorced from reality. When taking the emittance and energy spread into account, a view is that the beam energy spread will seriously undermine the coherence condition between the two undulator radiations with increasing of energy spread, especially for high-energy hard X-rays. A characteristic periods number is defined

by  $N_{c,n} = \frac{1}{5n} \left( \frac{\sigma_\gamma}{\gamma} \right)^{-1}$  and equivalent periods number

is defined by  $N_{ep} = 2N + \phi/2\pi$ . Where  $\phi$  is the phase slip between the two undulators. Coherence effects could clearly observed only when  $N_{c,n} \gg N_{ep}$  [2] or the intensity distribution presents a geometrical superposition of intensity from two independent source points at the center

of both undulators in the opposite case. The phase shifter has little effect in this case. However, it will see the conclusion is just opposite according to the work of this article later. Phase shifter is remain indispensable even if considering the effects of beam parameters.

To specify the performance of a synchrotron radiation (SR) source, photon flux density in the 4D phase space i.e. brilliance is the most common figure of merit. In general case, brilliance should be first calculated by the method of Wigner function [3] and then convoluted with the electron beam distribution in phase space to include the effects of emittance and energy spread. A widely used model to calculate the radiation brilliance from a single undulator is Gaussian approximation in the case of Gaussian electron beam distribution [4] which could help to simplify this calculation process. The only difference should be considered is that energy deviation of electrons will change the phase slip between the two undulators. Moreover, in most practical cases, it is sufficient to use on-axis brilliance to evaluated the SR performance. Therefore, we only calculate the on-axis brilliance in this paper.

## RADIATION MODEL OF DOUBLE UNDULATOR CONFIGURATION

To start with the calculation of the spectra of the combination of two undulators with the phase shifter between them analytically, we illustrate the whole structure in Fig. 1 [5]:

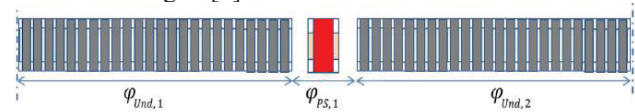


Figure 1: structure of the double undulator configuration.

Where  $\phi_{und,1}$  and  $\phi_{und,2}$  represent to the phase slip in each undulator.  $\phi_{ps}$  is the phase slip between the two undulator. We ignore the front-ends of the two undulators for it only cause an additional phase slip which contain in  $\phi_{ps}$ . The radiation field then is expressed by the sum of the two complex field emitted from both undulators as

$$E_{Double}(\omega, \theta, t) = \left[ 1 + e^{i(\phi_{und,1} + \phi_{ps})} \right] E_{Single}(\omega, \theta, t),$$

Where  $E_{single}$  denote the field emitted from a single undulator. And the on-axis radiation intensity is written as

# PREPARATION AND CHARACTERIZATION OF NON-EVAPORABLE Ti-Zr-V GETTER FILMS FOR HEPS\*

Ping He, Yong-Sheng Ma<sup>#</sup>, Yuchen Yang, Di-Zhou Guo, Baiqi Liu  
Institute of High Energy Physics, CAS, Beijing, China

## Abstract

For the low activation temperature and high pumping speed, surface pumping capacity, the TiZrV coatings were chosen to high energy photo source (HEPS). Films of TiZrV alloy have been deposited on 1.5 meter long, cylindrical vacuum chambers of 22mm diameter copper substrates in krypton ambient using DC magnetron sputtering system.

Film composition, the activation temperature and pumping properties have been investigated in order to optimize the deposition parameters for vacuum applications. The films were also studied using the X-ray photo-emission electron spectroscopy (XPS) after annealing them at different temperatures ranging from 180°C to 300°C for half hour in ultra-high vacuum environment.

Pumping speed and surface pumping capacity testing facilities were also being constructed to investigate the characterization of TiZrV.

## INTRODUCTION

The present work is being undertaken in the frame of Beijing Advanced Light Source project at Institute of High Energy Physics (IHEP). To further develop the technologies necessary for diffraction-limited storage rings based light source, it involves five areas: vacuum system/non-evaporative getter (NEG) coating of small chambers, injection/pulsed magnets, RF systems/bunch lengthening, magnets/radiation production with advanced radiation devices, and beam physics design optimization. By focusing the current beam to develop high brightness x-ray synchrotron, it requires beam lines in centimetre or even millimetre range in diameter in order to gain good control of beam position and shape. When the vacuum conductance is much reduced in such narrow chambers, they are difficult to reach ultrahigh vacuum (UHV) that is necessary for accelerators. Getter films deposited on the inner surface of the chamber would transform the vacuum chamber from an outgassing source into a pump.

The extensive use of NEG based pumping systems for large UHV systems, such as particle accelerators and Tokamak reactors, was pioneered by the European Organization for Nuclear Research (CERN) at the time of the design phase of the Large Electron Positron (LEP) collider [1 - 3]. The NEG strip covered about 23 of the 27 km of the LEP machine, providing vacuum in the range of 10e-10 Pa. Since then, SAES-Getters have made the NEG strip commercially available. NEG pumps contribute to the achievement of UHV in storage rings for particle physics

research and synchrotron radiation production, and are widely accepted by the accelerator community. In recent years [4 - 6], different getter materials have been investigated, Innovative vacuum pumps, based on the combination of sputter-ion pumps (SIPs) with NEG technology have been invented [7].

In this context, our work will focus on the progress of the deposition of NEG coatings in very narrow chambers, as well as engineering and physics challenges they face today.

## PREPARATION OF THE GETTER FILMS

A schematic diagram of the experimental setup for NEG deposition is shown in Fig. 1. The sample is a 1.5 m long, 22 mm in inner diameter copper cylindrical tube. The cathode was made by twisting three wires of high-purity (99.95%) titanium, vanadium and zirconium, each of 1 mm diameter. TiZrV type was chosen because of its lowest activation temperature among ternary getters.

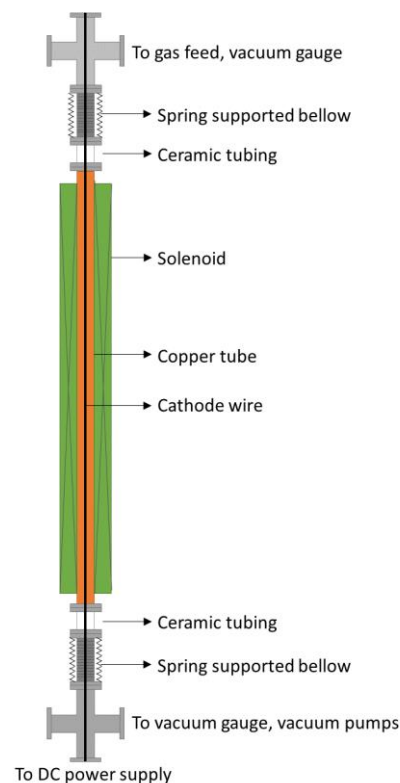


Figure 1: Schematic diagram of the experimental system for NEG deposition.

The tube sample is electrically isolated mounted to the chamber in the direction of gravity. The cathode wire runs through the tube sample and is positioned approximately

\* Work supported by IHEP  
<sup>#</sup>mays@ihep.ac.cn

# INFLUENCES OF HARMONIC CAVITIES ON THE SINGLE-BUNCH INSTABILITIES IN ELECTRON STORAGE RINGS

H. S. Xu\*, N. Wang

Key Laboratory of Particle Acceleration Physics and Technology,  
Institute of High Energy Physics, Chinese Academy of Sciences, Beijing, China

## Abstract

Single-bunch instabilities usually determine the bunch performance at high charges as well as the highest single-bunch currents in storage rings. It has been demonstrated that the passive harmonic cavities, which have been widely used in electron storage rings of the third-generation synchrotron light sources, can generally make the beam more stable. However, the influences of the harmonic cavities on the single-bunch instabilities are still not fully understood. We hereby present our study of both longitudinal and transverse single-bunch instabilities when using different settings of the harmonic cavities.

## INTRODUCTION

Harmonic cavities have been used to lengthen the bunches in the storage rings of many existing ring-based synchrotron light sources [1,2]. The increase of the Touschek lifetime due to the implementation of the harmonic cavities has been carefully studied and demonstrated in the operations of many machines [3–5]. Some studies show that the harmonic cavities help cure the longitudinal coupled-bunch instabilities [6–8]. Moreover, there are also some studies indicating that the harmonic cavities help stabilize the transverse coupled-bunch instabilities [9].

The newly proposed ultra-low emittance rings are usually more sensitive to the collective beam instabilities, while the total impedance of the rings tends to be higher since the much narrower vacuum chambers will be used. Therefore, people pointed out that it would be essential for the ultra-low emittance rings to implement the harmonic cavities to lengthen the bunches.

However, almost all of the existing harmonic cavities work in the 'passive' mode, meaning that no external RF power source will be used, the voltage in the harmonic cavities is induced only by the charged particle beam. In the operation mode with passive harmonic cavities, the voltage and phase of the RF field in the harmonic cavities would be determined mainly by charged particle beams. Therefore, it's non-trivial to optimize the settings of the passive harmonic cavities for different operation modes due to the lack of knobs. We are also considering to propose the active harmonic cavities in the HEPS storage ring for keeping the flexibility to optimize the settings of the harmonic cavities in different operation modes. Nevertheless, we need to understand better the influences of the harmonic cavities on the single-bunch instabilities first.

In the longitudinal direction, microwave instability is usually dominant. Studies of the microwave instability in both cases without and with ideal lengthening harmonic cavities have been reported for different machines. It would be interesting to carry out more studies between these two conditions. In the transverse direction, both the Transverse Mode-Coupling Instability (TMCI) and the head-tail instability could be the limiting factors. There hasn't been a universal explanation of the influences of the harmonic cavities on both the above mentioned transverse single-bunch instabilities. We hereby would like to carry out simulation studies of the above mentioned single-bunch instabilities. Our work will help understand the influences of the settings of the harmonic cavities. Hereby, we use the lattice and the impedance model loosely based on HEPS, the key parameters of which are listed in Table 1.

Table 1: Key Lattice Parameters Used in the Studies, which are Loosely Based on the HEPS

Parameters	Symbols	Values and Units
Circumference	C	1360.4 m
Beam Energy	$E_0$	6 GeV
Total Current	$I_0$	200 mA
Vertical Tune	$\nu_y$	106.16
Momentum Compaction Factor	$\alpha_c$	1.28e-5
Natural Energy Spread	$\delta_p/p$	1.14e-3
Average Radiation Energy Loss per Turn	U0	2.81 MeV
Harmonic Number of the Primary RF	$h_1$	756
Frequency of the Primary RF	$f_0$	166.60 MHz

The impedance model, consisting of most of the typical components, is shown in Figure 1. The simulations are mainly carried out by the `elegant` [10] and `Pelegant` [11] codes. Therefore, the convention used in Figure 1 is the same as the definition in `elegant`.

## HIGHER HARMONIC CAVITY

As mentioned in Table 1, we propose to use 166.60 MHz as the frequency of the primary RF cavities. The third harmonic cavity ( $\approx 500$  MHz) is chosen to provide bunch lengthening in our studies. If we consider using the active harmonic cavity, meaning that both the voltage and phase of the harmonic cavity can be adjusted freely, we can reach the

\* haisheng.xu@ihep.ac.cn

# UNDULATOR DEVELOPMENT ACTIVITIES AT DAVV-INDORE

Mona Gehlot, Roma Khullar, Geetanjali Sharma<sup>1</sup>, Jeevakhan Hussain<sup>2</sup>, G. Mishra  
 IDDL, School of Physics, DAVV, Indore-452001, India  
<sup>1</sup> Research Instruments GmbH, Gladbach, Germany  
<sup>2</sup> National Institute of Technical Teachers' Training and Research, Bhopal, India

## Abstract

Insertion Device Design Laboratory, DAVV has development activities on in-house design, fabrication and measurement of prototype undulators for synchrotron radiation and free electron laser application. The first prototype U50 was built with six periods, 50mm each period. It was PPM type. The next prototype U20 hybrid device based on NdFeB-Cobalt steel was built with aim to produce 0.24T to 0.05T in 10-20mm gap. The undulator is a 20mm period and there are 25 periods. The next one is U50-II PPM structure with 20 periods. In this paper we review the designs of all these undulators and briefly outline the user facilities of Hall probe bench, Pulsed wire bench and stretched wire magnetic measurement systems at IDDL.

## U 50 UNDULATOR

A planar undulator of Halbach Configuration made from Pure Permanent magnet type of NdFeB magnets named as U50 is design and developed in IDD lab DAVV [1]. One period is of 5 cm and there are six periods in a jaw and the total length of the undulator is 30cm. The undulator is a variable gap type. The minimum gap is 22 mm which can be varied up to 50mm. The magnet size is 12.5 mm × 12.5 mm × 50mm.

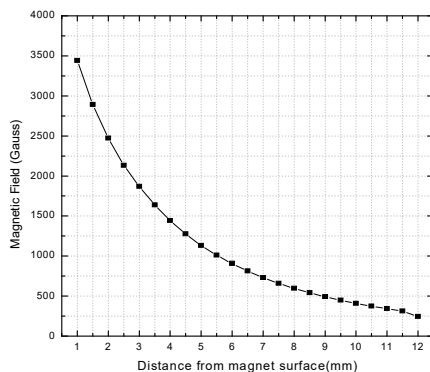


Figure 1: Magnetic field versus undulator gap for U50 undulator.

Figure.1 shows the graph for peak magnetic field with the variation in the distance from the surface of the undulator. At 1mm distance the field is around 3500Gauss.

The planar undulator was modify to a harmonic undulator by placing the shims on the required positions. We used CRGO shims for third harmonic undulator of

1.5 mm × 9.0 mm × 28 mm in thickness, height and length respectively. The shims fitted in the Perspex sheet will be place on the upper and lower jaw of the undulator. By using the same method we will also modify the wiggler for 5<sup>th</sup>, 7<sup>th</sup>, 9<sup>th</sup> harmonic undulator [2].

## U 20 UNDULATOR

It has completed the design of a hybrid undulator [3] and installed in the measurement bench for performance studies. U20 is a NdFeB based hybrid undulator with two NdFeB magnets and two poles per period. The undulator has twenty five periods and twenty mm each period length. The poles are made from Cobalt steel. The gap is variable from 10mm to 80mm. Fig.2 shows the radia model of U 20 undulator and Fig 3. Shows the schematic of arrangement of undulator in a jaw. The gap is manually driven by Ball screw arrangement. The maximum field is 3000Gauss at 10mm and  $\Delta B/B = 0.025$ . Figure 4 shows the photograph of the hybrid undulator with its support structure.

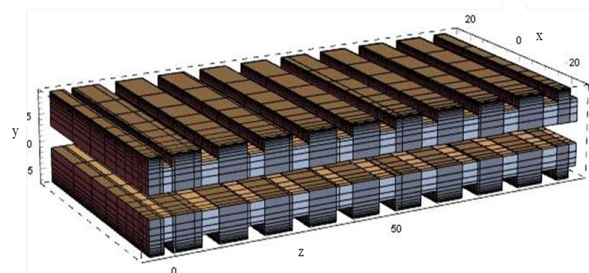


Figure 2: Radia model of U-20 undulator.

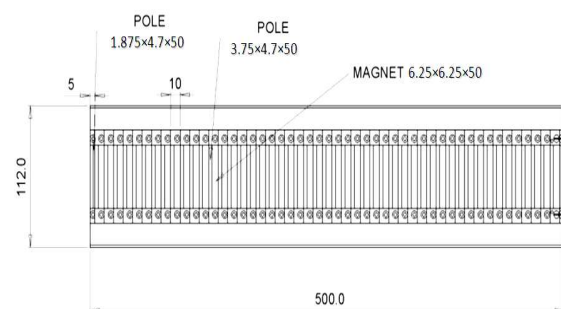


Figure 3: 0.5m Hybrid undulator design.

Content from this work may be used under the terms of the CC BY 3.0 licence (© 2018). Any distribution of this work must maintain attribution to the author(s), title of the work, publisher, and DOI.

# FEASIBILITY STUDY OF HIGH ENERGY X-RAY SOURCE AT PLS-II

Jang-Hui Han<sup>†</sup>, Jaeyu Lee, Sangbong Lee, Sojeong Lee, Tae-Yeon Lee  
 Pohang Accelerator Laboratory, Pohang, Korea

## Abstract

PLS-II operates for user service with the 34 beamlines since 2012. For engineering applications, especially for thick metal samples, a high energy X-ray beamline is under consideration to cover a photon energy up to 100 keV or beyond. By comparing the radiation spectra from various insertion devices types, superconducting wiggler was found to be a most promising candidate. A feasibility study to install the high field wiggler in the PLS-II ring is presented in this paper. Electron beam dynamics studies for a minimum impact on the electron beam parameters and engineering consideration to add more magnets are carried out.

## INTRODUCTION

Pohang Light Source II (PLS-II) operates for user service with synchrotron radiation ranging from IR to hard X-ray [1]. The electron beam energy is 3 GeV. The nominal beam current is 400 mA with top-up operation. The 282 m circumference ring has 12 cells. Each cell has two, 6.88 m long and 3.69 m short, straight sections. The ring have 24 straight sections in total. Twenty out of them are used for insertion devices, and the other straights are used for electron beam injection and RF cavities installation.

The main radiation source of PLS-II is the in-vacuum undulators with a period of 20 mm. The twenty in-vacuum undulators have a maximum magnetic field of 0.97 T when the magnet gap is 5 mm. One in-vacuum revolver undulator with four different periods, three APPLE-II type elliptically polarizing undulators and one out-vacuum undulator are in use. Two multipole wigglers with periods of 100 mm and 140 mm have maximum fields of 1.80 T and 2.02 T, respectively. The wigglers provide radiations up to 40 keV with a flux enough for users.

There is a request from users to provide higher energy X-rays for engineering applications. For instance, a high energy X-ray of 100 keV can be used to investigate a thick metal sample with a thickness of a few millimeters. A new insertion device for this purpose can be installed at the 2C slot which is empty at present. In this paper, we find the best insertion device type to generate a high energy X-ray with the electron beam parameters of PLS-II. We then study the feasibility to install the insertion device into the PLS-II ring with minimum impacts to the performance of the existing radiation sources.

## INSERTION DEVICE

Given the electron beam energy, a higher magnetic field generates an X-ray with higher photon energies. The critical

energy ( $\epsilon_c$ ) in keV varies with the magnetic field in T as  $\epsilon_c = 0.67E^2B$ , where E is the beam energy in GeV. To provide a sufficient flux at 100 keV, we need a critical energy of about 25 keV, which means a magnetic field of 4.2 T is required at the 3 GeV electron beam energy.

The flux densities from insertion devices under consideration, SCU16 (superconducting undulator with a 16 mm period) and SCW48 (superconducting wiggler with a 48 mm period), in addition to the existing ones, MPW10, MPW14 and IVU20, in PLS-II have been calculated by using the Spectra code [2] as shown in Fig. 1. A superconducting wiggler with a 4.2 T field and a 16 period can produce a flux density of more than one order of magnitude than the existing permanent magnet wigglers at the 100 keV photon energy. The parameters of the insertion devices used for the spectra calculation are summarized in Table 1.

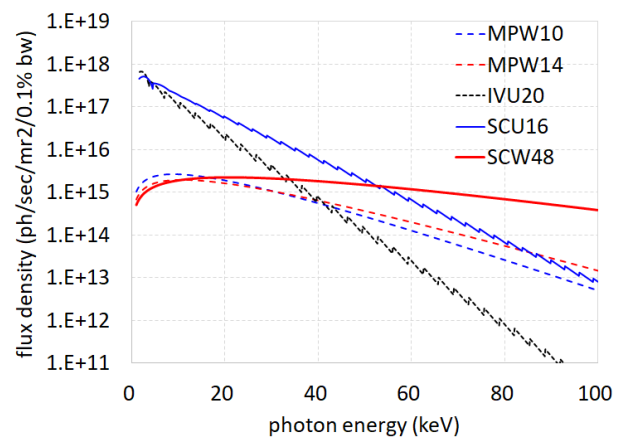


Figure 1: Spectra from insertion devices at PLS-II. At the 100 keV photon energy, a superconducting wiggler (SCW48) can provide a flux with more than an order of magnitude compared with the wigglers (MPW10 or MPW14) installed in the PLS-II ring.

Superconducting wigglers with a 4.2 T magnetic field are used at other synchrotron radiation sources [3]. Because of the available length of the 2C straight section, we consider a short SCW with a magnet length of about 0.8 m. In the 3.69 m long straight, a cryogenic tank to implement the SCW and additional quadrupole magnets for electron beam dynamics adjustment will be installed.

## IMPACT TO THE ELECTRON BEAM PARAMETERS

An insertion device with a high magnetic field can generate high flux at high photon energies. However, an insertion device with such a high magnetic field may deteriorate the electron beam emittance if that is placed at a position with

<sup>†</sup> janghui\_han@postech.ac.kr

# CONCEPTUAL DESIGN OF SUPERCONDUCTING TRANSVERSE GRADIENT UNDULATOR FOR PAL-XFEL BEAMLINE

S. Lee\*, J.-H. Han, Pohang Accelerator Laboratory, Pohang, Korea

## Abstract

Recently, the transverse gradient undulator (TGU) applications are suggested from laser plasma wake-field accelerator (LPWA) to ultimate storage ring (USR). Especially for X-ray FELs, TGU can be used to generate a large bandwidth radiation up to 10%. In this proceeding, a review of PAL-XFEL beam parameters and TGU requirements was done to apply a variable large bandwidth operation to the PAL-XFEL beamlines. Also, the conceptual design of TGU, based on superconducting undulator (SCU) was proposed, and B-field calculation results were introduced for large bandwidth operation modes of PAL-XFEL.

shows an undulator system parameters of each undulator systems.

Table 1: Undulator System Parameters of PAL-XFEL Beamlines

Parameters	HXU	SXU
Period	26.0 mm	35.0 mm
K	1.973	3.321
$B_{eff}$	0.812 T	1.016 T
$gap_{min}$	8.3 mm	9.0 mm
Length	5.0 m	5.0 m

## INTRODUCTION

The original TGU concept was introduced to overcome the large electron beam energy spread of an earlier stage of FEL development in the 1980s. The main parameter of TGU is the amount of K-value gradient in the transverse direction, defined by a parameter  $\alpha$ . The  $\alpha$  is defined as [1]

$$\alpha = \frac{\Delta K / K_0}{\Delta x} = \alpha_k / K_0. \quad (1)$$

Lately, the various types of TGU, canting pole geometry permanent undulator, and SCU were suggested and built for LPWA or USR to compensate the energy spread for compact FEL source development [2, 3]. Other TGU applications are also suggested for X-ray FEL by using a small energy spread electron beam [4]. This application uses a TGU and an RF deflecting cavity to generate the large bandwidth X-ray radiation. A deflected electron beam sees different K-values of TGU and the bandwidth of X-ray FEL can be adjusted by changing the gradient amount of TGU, up to 10% order. By using this scheme, FEL beamlines can provide a variable X-ray FEL bandwidth to meet the requirements of users.

The large bandwidth operation mode of PAL-XFEL requirements was calculated based on the suggested concept in Ref. [4] by using the PAL-XFEL beam and undulator parameters. The assumptions were used in this proceeding that a deflecting cavity is installed in front of the undulator beamlines and the TGU beamline, which can provide up to 10% bandwidth X-ray radiation, is installed. The deflected length of the electron beam was assumed as 1 mm for both the hard and soft X-ray beamlines for simple calculation. Table 2 shows a required K-value and gradient parameters to generate a 10% bandwidth radiation wavelength,  $\lambda_R$ , for the PAL-XFEL beamlines. For the calculation, the periods of the hard and soft X-ray TGUs were assumed as 26 mm and 35 mm, respectively.

Table 2: Undulator Parameters Required for 10% Large Bandwidth Operation of PAL-XFEL

Beamline	$\lambda_R$ (nm)	$K_0$	$\alpha_K (m^{-1})$	$\alpha (m^{-1})$
Hard	0.1	1.973	99.6	50.5
Hard	0.06	1.239	95.2	76.8
Soft	3	3.321	130.8	39.4
Soft	1	1.531	109.9	71.8

## LARGE BANDWIDTH MODE OF PAL-XFEL

### PAL-XFEL Beam Parameters

PAL-XFEL, an X-ray FEL user facility, has hard and soft x-ray beamlines based on Self Amplified Spontaneous Emission (SASE). The hard X-ray beamline uses a 10 GeV, 200 pC and 3.0 kA electron beam to provide 0.1 nm hard X-ray FEL by using twenty undulator units. For the soft X-ray beamline, seven undulator units are used to provide 1 nm soft X-ray FEL by using a 3.0 GeV, and 2.5 kA electron beam. Hard X-ray Undulator (HXU) and Soft X-ray Undulator (SXU) of PAL-XFEL are hybrid type undulators and Table 1

### Requirements for PAL-XFEL TGU

One of the important requirements of PAL-XFEL large bandwidth operation mode calculation was the variable bandwidth of X-ray FEL. To change the bandwidth of FEL, the TGU of PAL-XFEL can change the K-value and gradient by the user experiment requirements. Usually, the fixed gradient TGUs by using a canting pole geometry was proposed and built for the LPWA applications. These canting pole geometry TGUs can provide a fixed large gradient with a high K-value for short undulator periods. However, these canting pole geometry undulators are not proper for the PAL-XFEL large bandwidth operation mode.

\* sojung8681@postech.ac.kr

# BEYOND UNIFORM ELLIPSOIDAL LASER SHAPING FOR BEAM BRIGHTNESS IMPROVEMENTS AT PITZ

H. Qian<sup>#</sup>, J. Good, C. Koschitzki, M. Krasilnikov, F. Stephan, DESY, Zeuthen, Germany

## Abstract

In the last decades, photoinjector brightness has improved significantly, driven by the needs of free electron lasers and many other applications. One of the key elements is photocathode laser shaping for reducing emittance growth from nonlinear space charge forces. At the photoinjector test facility at DESY in Zeuthen (PITZ), a uniform flattop laser was used to achieve record low emittance for a bunch charge from 20 pC to 2 nC. Due to the ideal 3D space charge force linearization in ellipsoidal electron bunches, uniform ellipsoidal photocathode laser shaping were proposed to improve beam emittance up to 33% for 1 nC beam at PITZ. In this paper, we will show even further transverse emittance improvements in simulations for both flattop and ellipsoidal laser pulses with parabolic radial distribution, versus uniform distributions. The laser shaping effects on longitudinal phase space are also discussed.

## INTRODUCTION

Photoinjector development has seen great achievements in the past decades, enabling the success of X-ray free electron lasers (XFEL) and many other applications with high brightness electron sources. Besides high gradient gun and low thermal emittance cathode development, another key in improving photoinjector beam peak brightness is photocathode laser shaping for reducing emittance growth from nonlinear space charge forces. A temporal flattop laser pulse with uniform spatial distribution has been deployed at different photoinjectors to improve transverse beam emittance [1-3]. At the photoinjector test facility at DESY in Zeuthen (PITZ), a uniform flattop photocathode laser was used to achieve record low emittance for a bunch charge from 20 pC to 2 nC, fulfilling the nominal emittance specification of European XFEL injector.

Further improvement of state of the art photoinjector beam brightness is still wished by XFEL applications [4]. Besides going towards low bunch charge (<100 pC) for ultralow emittance (<0.1  $\mu\text{m}\cdot\text{rad}$ ), there is also a wish for improving high bunch charge (>0.5 nC) beam brightness for high flux FELs. For high bunch charge in a high gradient pulsed gun, or even low bunch charge in a low gradient CW gun, the beam is more vulnerable to the space charge effects, and uniform ellipsoidal photocathode laser shaping is proposed to further reduce the nonlinear space charge effect beyond uniform flattop laser shaping [5-7]. The argument is that an ellipsoidal bunch with a uniform density has 3D linearized space charge forces. Simulations based on the PITZ photoinjector have shown ~33% emittance reduction between uniform ellipsoidal laser pulses and uniform flattop laser pulses for 1 nC bunch

charge with ~50 A peak current [5]. Simulations based on LCLS-II CW injector have also shown ~33% emittance reduction with uniform ellipsoidal laser pulses for 100 pC bunch charge with 20 A peak current [6].

Compared to flattop laser shaping, uniform ellipsoidal laser shaping is more complicated due to the required 3D spatiotemporal control of the laser distribution. Generation of ellipsoidal photocathode laser pulses was first conceptually tested at ANL based on chromatic aberration of a dispersive lens, and is now under investigation at PITZ utilizing the Fourier masking technique [8, 9]. Besides 3D laser shaping, ellipsoidal electron beam was also demonstrated in blowout photoemission with longitudinal or transverse laser shaping only, but the optimum bunch charge is limited (~pC) [10, 11].

In this paper, we will first revisit the photoinjector simulation with uniform flattop and uniform ellipsoidal laser based on the PITZ injector. Then flattop and ellipsoidal laser pulses with parabolic spatial shaping instead of 3D uniform distribution is proposed to further improve photoinjector beam brightness, and their effects on both transverse and longitudinal phase spaces are discussed with simulation results.

## PITZ PHOTOINJECTOR SIMULATION

The PITZ gun is an L-band normal conducting gun for driving SC linac based FELs in pulsed mode. It features both high gradient (60 MV/m) and long RF pulse length (650  $\mu\text{s}$ ). A Cs<sub>2</sub>Te cathode is used to generate photoelectron bunch trains at 10 Hz. To characterize the gun and optimize beam emittance, the PITZ facility was established at DESY for FLASH and European XFEL, see Fig. 1. The maximum beam momentum after the booster is ~25 MeV/c, and the space charge effect is still not fully negligible for high bunch charge cases, so transverse projected emittance is measured with slit scan technique at ~0.9 m downstream the booster exit.

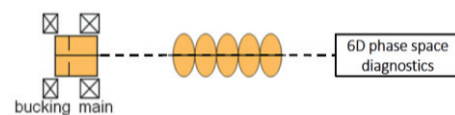


Figure 1: PITZ photoinjector layout.

In this paper, a MOGA tool developed at LBNL is used to drive ASTRA simulations for photoinjector optimization [12]. 10000 macro particles are used in MOGA simulations, and interesting solutions are refined with 200000 macro particles in ASTRA for detailed analysis. The PITZ injector layout is used as an example for investigating laser shaping effects on transverse emittance. The gun is set to 60 MV/m at maximum energy gain phase. The booster is set to maximum energy gain phase. The flattop laser is set to 22 ps FWHM with 2 ps edges, and the ellipsoidal laser is set

<sup>#</sup>houjun.qian@desy.de

# CONCEPTUAL DESIGN FOR SLS 2.0

M. Dehler, A. Streun, A. Citterio, T. Garvey, M. Hahn, L. Schulz, M. Negrazus, V. Vranković  
 PSI, Villigen PSI, Switzerland

## Abstract

After 17 years of user operation, we plan to do an upgrade of the Swiss Light Source (SLS) in the period 2023-2024. The entire storage ring will be replaced by a new layout allowing operation at emittances lowered by factors of 40-50. This is made possible by small aperture magnets allowing for a multi bend achromat design and - a special feature for SLS 2.0 - with reverse bends combined with longitudinal gradient bends (LGB) leading to zero dispersion at the maximum magnetic field, thus minimizing the quantum excitation of the beam due to synchrotron radiation. The compact magnet layout makes use of offset quadrupoles, combined function magnets and longitudinal gradient bends. All vacuum chambers along the electron beam path will be coated with a non-evaporable getter (NEG) film to ensure low photo-desorption and a quick vacuum conditioning. Numerical simulations of instability thresholds have been performed. We expect values on the order of 2 mA for the single bunch current.

## INTRODUCTION

Table 1: Main Parameters Of SLS 2.0 Compared To SLS

	SLS 2.0	SLS
Circumference [m]	290.4	288.0
Energy [GeV]	2.4	2.4
Current [mA]	400	400
Main RF frequency [MHz]	499.6	499.6
Nominal RF voltage [kV]	1420	2080
Harmonic number	484	480
Filling pattern gap	10%	19%
Damping times $\tau_{x,y,E}$ [ms]	4.9/8.4/6.5	8.6/8.6/4.3

The SLS started user operation in 2001 and has been operated in top-up mode since then. Today it is fully equipped with a set of 18 beam lines delivering about 5000 hours of user time per year with an excellent availability.

While it was state of the art at the time, a new generation of light sources are coming into operation or development, which make use of features such as advanced optics using low aperture magnets resulting in a dramatically reduced emittance. Given that the improved machine layout still needs to fit the existing facility with minimum changes, scaling existing designs, as e.g. for MAX-IV, would not have led to the required improvement in emittance of at least 30. A novel type of lattice was developed, which makes use of longitudinal gradient bends and reverse bends. At the price of stronger than anticipated modifications in the shielding walls and shifts in the source points of several beam lines, the old design with a three fold symmetry and three differ-

ent types of straights will be replaced by a strictly regular layout with twelve fold symmetry.

The low vacuum chamber aperture of 20 mm diameter used in the design poses challenges from two sides. Vacuum conductance along the chamber (worse by more than a factor five in comparison to SLS) becomes negligible, so that distributed pumping becomes essential. Also resistive effects leading e.g. to microwave instabilities need to be investigated closely. A comparison of the main parameters of the upgrade with the original SLS is shown in Table 1.

## OPTICS

The zero-current horizontal emittance in a storage ring is determined by the equilibrium between radiation damping and quantum excitation. The latter depends on the rate of photon emission, which is given by the strength of the magnetic field, and on the local dispersion function, because after emission of a photon, an electron starts an oscillation around the closed orbit corresponding to its reduced energy. The damping of horizontal oscillations thus excited is given by the total radiated power, which depends on the magnetic field strength, and by the horizontal ‘share’ of the overall damping, which is affected by transverse gradients in combined-function bending magnets.

The quantum excitation can be minimized by the use of longitudinal-gradient bends (LGBs, bending magnets for which the field varies along the beam path), while suppressing the dispersion at the LGB center, where the field is strongest. In a conventional periodic cell, this would lead to an over-focusing of the transverse beta function  $\beta_x$ , since also the bending magnets have a defocusing effects on the dispersion. This can be solved by the use of small reverse bends (RBs), realized in the SLS 2.0 lattice by generating the reverse kicks by a transverse offset of the horizontal-focusing quadrupoles nearby.

A welcome effect of this strategy is the enhanced radiation damping. The field variation in the LGB increases the radiated power compared to classical homogeneous bending magnets. In addition, the reverse bends increase the total absolute bending angle to values larger than  $360^\circ$ . Altogether, a lattice cell combining LGBs and RBs can provide up to a five times lower equilibrium emittance compared to a conventional cell [1].

Figure 1 shows the fundamental building block of the lattice, a cell consisting of a center LGB with adjacent vertically focusing bends (VB) and two reverse bends. Five full and two half LGB-RB cells form one of the twelve identical 7-bend achromat arcs (7BAs) as shown in Fig. 2. Some cells will use LG-superbends of up to 6 Tesla peak-field [2] instead of the normal LGBs in order to provide x-rays in the 50 to 100-keV range. Table 2 compares the main parameters of

# STATUS OF CAEP THz FREE ELECTRON LASER OSCILLATOR\*

D. Wu, M. Li<sup>†</sup>, X. F. Yang, X. Luo, X. M. Shen, D. X. Xiao, J. X. Wang, P. Li, X. K. Li, K. Zhou, C. L. Lao, P. Zhang, Y. Xu, S. F. Lin, Q. Pan, L. J. Shan, T. H. he, H. B. Wang  
 Institute of Applied Electronics, China Academy of Engineering Physics (CAEP/IAE),  
 Mianyang, 621900, P.R.China

## Abstract

China Academy of Engineering Physics tera-hertz free electron laser (CAEP THz FEL, CTFEL) is the first THz FEL oscillator in China, which was jointly built by CAEP, Peking university and Tsinghua university. The stimulated saturation of the CTFEL was reached in August, 2017. This THz FEL facility consists of a GaAs photocathode high-voltage DC gun, a superconducting RF linac, a planar undulator and a quasi-concentric optical resonator. The terahertz laser's frequency is continuous adjustable from 2 THz to 3 THz. The average power is more than 10 W and the micro-pulse power is more than 0.1 MW.

## INTRODUCTION

Free electron laser (FEL) can be the most powerful tool as tera-hertz power source. It has many advantages, such as monochrome, high-power, linear-polarization, continuously-tunable frequency. A lot of FEL facilities, such as ELBE in Germany [1], FELIX in Holland [2], UCSB in the USA [3] and NovoFEL in Russia [4], have played important roles in the THz sciences. In the near future, of the 20 FEL facilities planned to be built in the whole world, there will be at least 8 ones operating in the THz range [5].

CAEP THz FEL (CTFEL) facility is the first high average THz source based on FEL in China [6, 7], which is driven by a DC gun with a GaAs photocathode [8, 9] and two 4-cell 1.3 GHz super-conducting radio frequency (SRF) accelerator [10]. The repetition of CTFEL is 54.167 MHz, one in twenty-fourth of 1.3 GHz. The effective accelerator field gradient is about 10 MV/m. The terahertz wave frequency is continuous adjustable from 2 THz to 3 THz. The average power is more than 10 W and the micro-pulse power is more than 0.1 MW. This paper gives an introduction of this facility and its THz laser characters.

## FACILITY COMPONENTS

### Overview

Figure 1 shows the layout of the CTFEL facility. High average power high-brightness electron beam emits from the high-voltage DC gun equipped with a GaAs photocathode. The beam is then accelerated by a 2×4-cell RF superconducting accelerator and gain a kinetic energy from 6 MeV to 8 MeV. Passing through an achromatic section, the beam

then goes into the undulator magnet field and generate the spontaneous radiation. The radiation resonates in the THz optical cavity and reaches saturations.

Table 1 gives more information of the electron beam. The accelerator is designed to operate in both CW and macro-pulse mode. It is now working in macro-pulse mode in the first step. The typical output in this “step one” is in 1 ms and 1Hz macro-pulse mode. The duty cycle will update to >10% in 2018 as the “step two”. And the CW operation will be reached in the “step three”.

Table 1: Electron Beam Parameters

Parameters	Designed value	Unit
Bunch charge	10~100	pC
Micro-pulse repetition	54.167	MHz
Macro-pulse repetition	1~20	Hz
Duty cycle	$10^{-5} \sim 1$	
Kinetic energy	6~8	MeV
Normalized emittance	<10	$\mu\text{m}$
Micropulse length	4~8	ps
Energy spread	<0.75	%

### High-voltage DC Electron Source

Figure 2 shows the system of the high-voltage DC electron source, which consists of a photocathode preparation chamber, a load-lock system, a drive laser, a high-voltage DC gun and some beam elements such as three solenoids and an RF buncher. The electron source can provide 320 keV high brightness beams both in CW mode and in macro-pulse mode. The average current has reached 1 mA 5 mA. The micro-pulse length is compressed to 8 ps by the RF buncher.

### RF Superconducting Accelerator

Owing to the advantages of superconducting RF technology in CW mode operation, a 2×4-cell superconducting linac module has been adopted to accelerate 320 keV, 1~5 mA electron beams from the DC-gun up to an energy of 6~8 MeV. The 2×4-cell module is composed of two SRF cavities, two power couplers, two tuners and a cryostat, as shown in Fig. 3. With the goal of 5 mA, 54.17 MHz CW beams, the components have been designed accounting for higher-order modes (HOMs), beam loading and cryogenic issues. The phase stability of the low-level RF control system is 0.1°, and the amplitude stability is better than 0.05%. After the acceleration, the normalized emittance of the beam is less than 8 mm-mrad, and the relative energy spread is less than 0.2%.

\* Work supported by China National Key Scientific Instrument and Equipment Development Project (2011YQ130018), National Natural Science Foundation of China with grant (11475159, 11505173, 11575264 and 11605190)

<sup>†</sup> liming@caep.cn

# GPT-CSR: A NEW SIMULATION CODE FOR CSR EFFECTS

S.B. van der Geer<sup>†</sup>, M.J. de Loos, Pulsar Physics, Eindhoven, The Netherlands  
 I.D. Setija, P.W. Smorenburg, ASML, Veldhoven, The Netherlands

P.H. Williams, STFC Daresbury Laboratory and Cockcroft Institute, Warrington, United Kingdom

## Abstract

For future applications of high-brightness electron beams, including the design of next generation FEL's, correct simulation of Coherent Synchrotron Radiation (CSR) is essential as it potentially degrades beam quality to unacceptable levels. However, the long interaction lengths compared to the bunch length, numerical cancellation, and difficult 3D retardation conditions make accurate simulation of CSR effects notoriously difficult. To ease the computational burden, CSR codes often make severe simplifications such as an ultra relativistic bunch travelling on a prescribed reference trajectory. Here we report on a new CSR model, implemented in the General Particle Tracer (GPT) code [1], that avoids most of the usual assumptions: It directly evaluates the Liénard–Wiechert potentials based on the stored history of the beam. It makes no assumptions about reference trajectories, while also taking into account the transverse size of the beam. First results demonstrating microbunching gain in a chicane are presented.

## INTRODUCTION

Here we add a new alternative to the list of simulation codes for CSR effects. Our version is implemented in the GPT code, and we intentionally steered away from the approaches used by other codes such as Elegant [2,3]. The goal we had in mind was not to create the ‘best’ CSR code per-se; we wanted to make a model that could answer the question what the consequences are of the assumptions made by the already existing codes. In order to do so, we created a code that is based on direct evaluation of the retarded Liénard–Wiechert potentials.

The main approximation used in this GPT element is that the bunch is modeled as a parametric curve, sliced in the direction of average propagation. This is typically a very good approximation because the dynamics of the underlying process are governed by the rest-frame properties of the bunch. In this frame, the bunch is elongated by the Lorentz factor compared to the length in the laboratory frame, resulting in a very narrow ribbon of charge. In this GPT model, the ribbon itself is allowed to meander through 3D space, capturing the largest amount of 3D effects possible within the parametric 1D framework. The chosen approach makes use of the fact that if all individual beam segments that have radiated in the past are stored, this information is sufficient to calculate the electromagnetic fields everywhere in 3D space, at any later point in time.

The result of the chosen approach is that changes in bunch shape between the point where radiation is emitted and the interaction point are properly taken into account. Another advantage is that the usual ultra relativistic assumptions are not needed. A conceptual simplification compared to some other codes is that the radiation is

emitted based on the derivative of the momentum, regardless of the reason: A very strong electrostatic deflection field will give rise to the same emitted radiation as a bend-magnet or a heavily misaligned quadrupole as long as the trajectories are the same. Furthermore, because the element is based on electromagnetic fields and not ‘effects’, radiation fields and the fields of other beamline components can all be correctly added. This allows for beamline components very close to the exit of a bend magnet, where a strong CSR wake can be travelling almost parallel to the bunch over long distances, to be properly simulated without degrading the accuracy of the CSR calculations. Finally, both the transverse and longitudinal fields are calculated, taking into account not only energy changes but also transverse effects that might vary along the bunch causing projected emittance growth.

The implementation of this element consists of two main parts: A history manager that maintains the history of the bunch, and a field calculator that integrates the radiation fields based on this stored history. They will be described in the following sections. We end by showing first simulation results, followed by a conclusion.

## HISTORY MANAGER

The history manager of our new CSR code stores at discrete time intervals a 1D parameterization of the entire bunch, including basic information about transverse size. The first step is to switch to a new coordinate system, where  $\mathbf{u}$  is the average direction of propagation,  $\mathbf{v}$  lies in the bend-plane, and  $\mathbf{w}=\mathbf{u} \times \mathbf{v}$ . In this frame, an estimate of the current profile is obtained by slicing in  $\mathbf{u}$ , and this in turn defines the non-equidistant charge quantiles of the beam. The recipe is shown schematically in Figure 1.

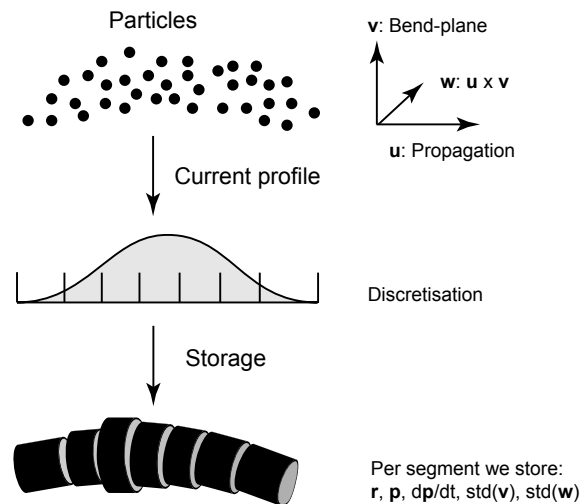


Figure 1: Schematic of the CSR history manager.

<sup>†</sup> info@pulsar.nl

# IMPEDANCE EVALUATION OF PF IN-VACUUM UNDULATOR (IVU) WITH THEORIES AND SIMULATIONS AND EXPERIMENTAL CONFIRMATION OF THEM BY THE TUNE MEASUREMENT

O. Tanaka<sup>†</sup>, N. Nakamura, T. Obina, and K. Tsuchiya, High Energy Accelerator Research Organization (KEK), Tsukuba, Japan

## Abstract

Four In-Vacuum Undulators (IVU) were recently installed to Photon Factory (PF) at KEK. The estimate of their impedance and kick factors is a very important issue, because they could considerably increase the total impedance of PF. Moreover, the coupling impedance of the IVUs could lead to the beam energy loss, changes in the bunch shape, betatron tune shifts and, finally, to the various beam instabilities. Using the simulation tool (CST Particle Studio), longitudinal and transverse impedances of the IVUs were evaluated and compared to analytical formulas and measurement results. The study provides guidelines for mitigation of unwanted impedance, for an accurate estimate of its effects on the beam quality and beam instabilities and for the impedance budget of a newly designed next-generation machine which has many IVUs and small-aperture beam pipes.

## INTRODUCTION

Accelerator components can interact with bunched particles through their inducing wake fields and impedance. Impedances lead to unwanted effects such as beam energy loss, changes in the bunch shape, betatron tune shifts, and to the various beam instabilities. Knowledge of impedances of the accelerator components is of a great importance because it allows to improve the performance the accelerator essentially. Therefore, they should be carefully estimated and evaluated in the very beginning of the design process of any high intensity machine.

At KEK Photon Factory (PF) light source, we have four newly installed In-Vacuum Undulators (IVUs). The IVU's vacuum chamber has a complex geometry. It consists of two taper transitions between the undulator and the beam chamber, one copper plate on the undulator magnets for RF shielding of the magnets from a beam, and two step transitions between the octagon and the taper region. Each part makes its own impact on the total frequency dependent impedance of the entire IVU. Design issues of IVU including taper regions, undulator plates and step transitions are well-studied (see, for example, [1 – 4]). Such Insertion Devices (IDs) are known to make small impacts on the total impedance of a machine [5]. However, the PF IVUs were installed much after the construction of the ring itself was completed, and there was a need of the proper IVU's impedance evaluations.

To quantify IVUs induced impedance we engaged both a powerful simulation tool (Wakefield Solver of CST Particle Studio [6]), and theoretical assessments (for

cross-checking the results of simulation), and, finally, an experimental reconciliation of the impedance values obtained from our studies. Such a comprehensive analysis shown in this article will be a standard procedure for the design of new accelerators. It allows to predict the thresholds of instabilities and to assess the influence of collective effects [7 – 8].

A few decades ago only 2D modeling of devices with axial symmetry was available. And to evaluate the impedances of real sections of the accelerator, scientists had to rely entirely on the results of the measurements [9]. Nowadays 3D impedance simulation tools (CST Particle Studio, GdfidL, MAFIA, etc.) have comparably good reliability and improved performance. Therefore, they provide an ability to simulate IDs and accelerator components with their full geometries. For example, at PETRAIII the wakefields of the whole IVU vacuum vessel were evaluated, although it required a considerable computing powers [2]. In the process of simulation of wakefields and impedances, the attention of scientists has been gradually shifted to the consideration of chamber shapes different from the circular geometry (rectangular, elliptical). Thus, we began to distinguish between dipolar (or driving) and quadrupolar (or detuning) contributions to the transverse impedance, whereas only impedance of the dipole mode has been studied previously. This new treatment gives an advantage to obtain different impedance effects on the beam dynamics. Namely, the dipolar wake provides an information about instabilities growth rate. And quadrupolar wake impacts on incoherent effects such as emittance growth and damping. This approach is a courtesy of CERN impedance group [10 – 11].

In this study we show how we identify the major impedance contributors and evaluate their impedance using theoretical formulas, CST Studio simulations and measurements. The KEK future light source will include one IVU for each lattice cell, therefore many IVUs are planned to be installed. Evaluation and improvement of their impedance is one more target of the present study. Now, let us discuss the details of these impedance evaluations, and its experimental confirmation.

## IMPEDANCE EVALUATION FOR PF IVU BY SIMULATIONS AND THEORY

The PF IVU consists of three parts (see Fig. 1 a) – c)). Each of these parts impacts on the total impedance of the IVU. They are:

- Taper between the flange and the undulator (200  $\mu\text{m}$  thick) for the geometrical impedance.

<sup>†</sup> olga@post.kek.jp

## AN OVERVIEW OF THE PROGRESS ON SSMB

Chuanxiang Tang\*, Xiujie Deng†, Wenhui Huang, Tenghui Rui,  
Alex Chao<sup>1</sup>, Tsinghua University, Beijing, China

<sup>1</sup> also at SLAC, Menlo Park, USA

Jörg Feikes, Ji Li, Markus Ries, HZB, Berlin, Germany

Arne Hoehl, PTB, Berlin, Germany

Daniel Ratner, SLAC, Menlo Park, USA

Eduardo Granados, CERN, Geneva, Switzerland

Chao Feng, Bocheng Jiang, Xiaofan Wang, SINAP, Shanghai, China

### Abstract

Steady State Microbunching (SSMB) is an electron storage ring based scheme proposed by Ratner and Chao to generate high average power coherent radiation and is one of the promising candidates to address the need of kW level EUV source for lithography. After the idea of SSMB was put forward, it has attracted much attention. Recently, with the promote of Chao, in collaboration with colleagues from other institutes, a SSMB task force has been established in Tsinghua University. The experimental proof of the SSMB principle and a feasible lattice design for EUV SSMB are the two main tasks at this moment. SSMB related physics for the formation and maintenance of microbunches will be explored in the first optical proof-of-principle experiment at the MLS storage ring in Berlin. For EUV SSMB lattice design, longitudinal strong focusing and reversible seeding are the two schemes on which the team focuses. The progresses made as well as some challenges from physical aspects for EUV SSMB will be presented in this paper.

### INTRODUCTION

Storage ring based synchrotron radiation facilities and linac based free electron lasers are the main workhorses of nowadays accelerator light sources and deliver light with characteristics of high repetition rate and high peak power respectively. However, there are some applications demanding high average power. One example is the kW level 13.5 nm EUV source needed by semiconductor industry for lithography. To generate high average power radiation, high repetition rate or high peak power alone is not enough, we need to combine both. This hope of combination leads to the idea of SSMB [1], i.e. microbunching in a steady state, microbunching for high peak power and steady state for high repetition rate.

It can be seen from the introduction above that SSMB is a general concept and there are several different specific scenarios proposed since the first publication. Interested readers may read [1-5] for more details about these scenarios. As a new accelerator physics idea, SSMB has attracted a lot of attention. Recently, with the promote of Chao, in collaboration with colleagues from other institutes, a SSMB task force

has been established in Tsinghua University with a final goal of kW level EUV source. The two main tasks at this moment are the experimental proof of the SSMB principle and a feasible lattice design for EUV SSMB. The PoP experiment is planned based on the Metrology Light Source (MLS) [6], the radiation source of the German national metrology institute (PTB). The possibility of conducting the experiment on MLS is being carefully evaluated. For the eventual EUV SSMB lattice design, longitudinal strong focusing and reversible seeding are the two schemes being pursued by the team. The progresses made as well as challenges encountered in the study will be given below.

### STRONG FOCUSING SSMB

The natural idea of SSMB is a scaling from microwave to optical, i.e. using laser modulator to form optical buckets to microbunch the electron beam just like using RF to bunch electron beam in traditional storage rings.

One of the SSMB lattice scheme is the longitudinal strong focusing scheme. In the strong focusing scheme, a low alpha lattice is needed to let the beam microbunch in the optical buckets in a steady state. However, it is difficult to realize nm level microbunches needed for coherent EUV radiation by applying low alpha lattice alone due to challenges to be introduced momentarily. Longitudinal strong focusing will be applied to compress the bunch length further for coherent EUV generation. Two modulators sandwiching one radiator will play the role of longitudinal strong focusing not unlike the function of final focusing cell in a collider on the transverse dimension. Figure 1 shows the schematic configuration and the longitudinal phase space evolution of one strong focusing SSMB super-period.

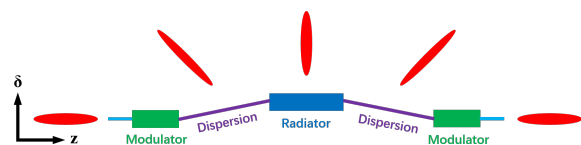


Figure 1: One super-period of longitudinal strong focusing.

In the reversible seeding scheme [3], on the other hand, there is no need of a low alpha lattice. The reversible seeding scheme is also investigated by the collaboration. We will start with the introduction of strong focusing SSMB.

\* tang.xuh@tsinghua.edu.cn

† dxj15@mails.tsinghua.edu.cn

# TRANSPARENT LATTICE CHARACTERIZATION WITH GATED TURN-BY-TURN DATA OF DIAGNOSTIC BUNCH-TRAIN

Y. Li, W. Cheng\*, K. Ha and R. Rainer,  
Brookhaven National Laboratory, Upton, New York 11973 USA

## Abstract

Methods of characterization of a storage ring's lattice have traditionally been intrusive to routine operations. More importantly, the lattice seen by particles can drift with the beam current due to collective effects. To circumvent this, we have developed a novel approach for dynamically characterizing a storage ring's lattice that is transparent to operations. Our approach adopts a dedicated filling pattern which has a short, separate Diagnostic Bunch-Train (DBT). Through the use of a bunch-by-bunch feedback system, the DBT can be selectively excited on-demand. Gated functionality of a beam position monitor system is capable of collecting turn-by-turn data of the DBT, from which the lattice can then be characterized after excitation. As the DBT comprises only about one percent of the total operational bunches, the effects of its excitation are negligible to users. This approach allows us to localize the distributed quadrupolar wake fields generated in the storage ring vacuum chamber during beam accumulation. While effectively transparent to operations, our approach enables us to dynamically control the beta-beat and phase-beat, and unobtrusively optimize performance of National Synchrotron Light Source-II accelerator during routine operations.

## INTRODUCTION

For high brightness synchrotron light sources, it is essential to mitigate lattice distortion to optimize performance during routine operations. At National Synchrotron Light Source-II (NSLS-II) [1], the deviation of the linear lattice has been observed but not quantitatively characterized during operations. Although there are several methods to characterize and correct the linear lattice during dedicated machine studies periods, they often interfere with stable beam conditions due to the magnitude of beam manipulation for lattice characterization. Common tools used for lattice characterization and/or correction include, but are not limited to: Linear Optics from Closed Orbit (LOCO) [2,3], TbT data of a short bunch-train excited by a short pulse excitation [4–9], or a long bunch-train excited by the bunch-by-bunch feedback system [10].

With modern advancements in BPM technology, storage ring lattices can be characterized with accurately aligned BPM turn-by-turn (TbT) data. To accomplish this, the beam is excited with a pulsed magnet, also known as a “pinger” magnet. At most light source facilities, however, the pulse width of a pinger wave usually lasts several micro-seconds, while the separation between two adjacent buckets is a few nanoseconds. Most of existing BPM systems are unable to

resolve the bunch-by-bunch signals. The TbT data that reveals the centroid motion of the long bunch-train is therefore highly decoherent after excitation [11–13]. To obtain clean TbT data with such a long pulse width, one would need to utilize a shorter bunch-train. Or one could utilize a well designed pulsed magnet with a wide flat top waveform [14].

Another method of exciting long bunch-trains with a bunch-by-bunch feedback system (BBFB) has been developed at Diamond light source [10]. The excitation amplitudes are small (significantly less than the beam size) but at high frequencies. Their method involves collecting the TbT data with dedicated signal processing, after excitation. To characterize the lattice during operations, however, requires excitation of the whole operational bunch train. To achieve comparable resolution as the pinger excitation technique, their method also requires continuous excitation of the whole operational bunch train. Hereby, our method introduces a more transparent technique for lattice characterization that utilizes a short diagnostic bunch-train (DBT) developed at NSLS-II [15]. The DBT is isolated from the main user bunch-train and transversely excited with the BBFB system [16]. The TbT data of the DBT is collected using the gated functionality of BPMs. As the DBT (10 bunches) comprises only about one percent of the total bunches, and the excitation amplitude is less than 1 millimeter, the effects on the global beam motion are negligible to users. Additionally, an “on-demand” triggering mode is utilized to minimize the disturbance on the circulating beam. With minimal beam disturbance, this approach is effectively transparent to the beamlines and can be applied at any time during operations without interfering with experiments, even ones requiring high sensitivity.

## SELECTIVE BUNCH EXCITATION AND GATED TBT DATA ACQUISITION

This section discusses the necessary requirements for lattice characterization by designing a technique which utilizes a dedicated filling pattern configuration, gated bunch-train excitation and data acquisition.

### *Diagnostic Bunch-Train (DBT)*

During routine operation, various collective instabilities are suppressed by the transverse BBFB system. High precision lattice characterization, however, requires beam excitation which the BBFB would normally prevent. To bypass this, a short DBT is filled and is separated from the main, long operational bunch-train (see Fig. 1). The BBFB can be configured to only stabilize the operational bunch train, and not the DBT. The separation between the DBT and the

\* W. Cheng and Y. Li contributed equally to this work

# LASER SEEDING OF ELECTRON BUNCHES FOR FUTURE RING-BASED LIGHT SOURCES\*

S. Khan<sup>†</sup>, B. Büsing, N. M. Lockmann, C. Mai, A. Meyer auf der Heide,  
 B. Riemann, B. Sawadski, M. Schmutzler, P. Ungelenk

Zentrum für Synchrotronstrahlung (DELTA), TU Dortmund, 44227 Dortmund, Germany

## Abstract

In contrast to free-electron lasers (FELs), ring-based light sources are limited in intensity by incoherent emission and in pulse duration by their bunch length. However, FEL seeding schemes can be adopted to generate intense and ultrashort radiation pulses in storage rings by creating laser-induced microbunches within a short slice of the electron bunch. Microbunching gives rise to coherent emission at harmonics of the seed wavelength. In addition, terahertz (THz) radiation is coherently emitted. At the 1.5-GeV electron storage ring DELTA, coherent harmonic generation (CHG) with single and double 40-fs pulses is routinely performed at seed wavelengths of 800 and 400 nm. Seeding with intensity-modulated pulses to generate tunable narrow-band THz radiation is also performed. As a preparation for echo-enabled harmonic generation (EEHG), simultaneous seeding with 800/400-nm pulses in two undulators has been demonstrated. In addition to short-pulse generation, steady-state microbunching at ring-based light sources will be discussed.

## INTRODUCTION

Synchrotron light sources based on electron storage rings are and will continue to be the workhorses to investigate the structure of matter on the atomic scale with photons in the vacuum-ultraviolet (VUV) to X-ray range [1]. Over half a century, remarkable progress has been made regarding intensity in terms of photon flux and brilliance as well as stability of the photon beams. With the MAX IV facility in Lund/Sweden, another step was taken in reducing the horizontal beam emittance by introducing a 7-bend achromat lattice [2], and other facilities have upgrade plans in the same direction.

In contrast to conventional synchrotron light sources, free-electron lasers (FELs) achieve extremely high average and peak brilliance by using electron beams from linear accelerators (linacs) and by microbunching which gives rise to coherent emission of radiation [3]. While the beam in a storage ring is subject to a long-term equilibrium between radiation excitation and damping, the electron bunches in a linac exist only for a few microseconds and retain the small emittance and bunch length with which they are produced. A bunch length being orders of magnitude smaller than in a storage ring implies a high peak current which makes high-gain FEL amplification possible. In addition, the short pulse

length of emitted radiation allows to study the dynamics of matter with a temporal resolution in the femtosecond regime.

The spectral power of radiation emitted by  $n_e$  electrons at frequency  $\omega$  is given by [4]

$$\begin{aligned} P(\omega) &= n_e^2 \cdot \left| \frac{1}{n_e} \sum_{j=1}^{n_e} e^{-i\omega t_j} \right|^2 \cdot P_e(\omega) \\ &= n_e^2 \cdot b^2(\omega) \cdot P_e(\omega) \\ &= n_e \cdot P_e(\omega) + \left| \sum_j \sum_{k \neq j} e^{i\omega(t_j - t_k)} \right| \cdot P_e(\omega) \\ &= n_e \cdot P_e(\omega) + n_e(n_e - 1) \cdot g^2(\omega) \cdot P_e(\omega), \end{aligned} \quad (1)$$

where  $P_e(\omega)$  is the spectral power emitted by one electron,  $b^2(\omega)$  is the bunching factor and  $g^2(\omega)$  is the so-called form factor. Thus,  $P(\omega)$  is proportional to  $n_e$  for randomly distributed electrons as in storage rings but has a component proportional to  $n_e^2$  if the longitudinal distribution has a significant Fourier contribution at frequency  $\omega$ . As sketched in Fig. 1, this is achieved by structures of the order of the wavelength  $\lambda = c/\omega$ , either (i) by a sufficiently short bunch, (ii) by a short dip in the longitudinal distribution (iii) by an instability with fluctuations of the electron density, or most efficiently (iv) by periodic microbunching.

A storage ring with microbunched electrons would combine the high repetition rate and stability of SR sources with the high radiation power of an FEL. These benefits have already been demonstrated, e.g., in the coherent emission of terahertz (THz) radiation at storage rings in low-alpha operation where the bunch length can be reduced to the order of 1 ps [5]. However, this example also shows a limiting peculiarity of storage rings, namely the so-called longitudinal microwave instability (or turbulent bunch lengthening) which causes the bunch length to increase above a given threshold of the bunch charge.

For short-wavelength radiation, the periodic microbunching of a short fraction (a “slice”) of a long electron bunch gives rise to coherent emission of an equally short radiation pulse which can be employed for time-resolved studies in pump-probe experiments where, e.g., a laser pulse excites the sample and a short-wavelength pulse probes its state as a function of the delay between the two pulses [6]. Here, the time resolution depends on the lengths of both pulses and on the stability of the delay.

Starting from a random electron distribution in longitudinal phase space, microbunching requires a manipulation of

\* Work supported by BMBF (05K16PEA, 05K16PEB), MERCUR (Pr-2014-0047), DFG (INST 212/236-1 FUGG) and the Land NRW.

<sup>†</sup> shaukat.khan@tu-dortmund.de

# COMPACT ARC COMPRESSOR FOR FEL-DRIVEN COMPTON LIGHT SOURCE AND ERL-DRIVEN UV FEL\*

S. Di Mitri, <sup>†</sup>, Elettra – Sincrotrone Trieste S.C.p.A., 34149 Basovizza, Trieste, Italy  
 I. Akkermans, I. Setjia, ASML Netherlands B.V. Technology, 5501 Veldhoven, The Netherlands  
 D. Douglas, Thomas Jefferson National Accelerator Facility, Newport News, VA 23606, USA  
 C. Pellegrini<sup>1</sup>, SLAC National Accelerator Laboratory, Menlo Park, CA 94025, USA  
 G. Penn, M. Placidi (retired), Lawrence Berkely National Laboratory, Berkeley, CA 94720, USA  
<sup>1</sup>also at University of California, Los Angeles, CA 90095, USA

## Abstract

Many research and applications areas require photon sources capable of producing extreme ultra-violet (EUV) to gamma-ray beams with reasonably high fluxes and compact footprints. We explore the feasibility of a compact energy-recovery linac-driven EUV free electron laser (FEL), and of a multi-MeV gamma-rays source based on inverse Compton scattering from a high intensity UV FEL emitted by the electron beam itself. In the latter scenario, the same electron beam is used to produce gamma-rays in the 10-20 MeV range and UV radiation in the 10-15 eV range, in a  $\sim 4 \times 22 \text{ m}^2$  footprint system.

## MOTIVATIONS

This work recalls design strategies for the minimization of Coherent Synchrotron Radiation (CSR) instability [1] in high brightness electron beams time-compressed in compact multi-bend lattices, i.e., compressive arcs. Two examples are given: a compact Energy Recovery Linac (ERL)-driven Free-Electron Laser (FEL) for production of  $\sim 100 \text{ W}$  average FEL power in EUV [2], and a compact FEL-driven Inverse Compton Scattering (ICS) light source devoted to geo-archaeology [3]. The ERL-FEL design targets a cost-effective method of producing integrated circuits and high-volume microchips through nanolithography. The FEL-ICS design aims at the generation of  $\sim 10 \text{ MeV}$  range photons in a compact footprint, for applications in computed tomography of cultural heritage and medical diagnostics.

## COMPACT ERL-FEL

### Overview

Figure 1 sketches a compact non-recirculating ERL-FEL, whose footprint is approximately  $20 \times 50 \text{ m}^2$ . Table 1 lists the main parameters of the facility. The linear bunch length compression factor to be exploited in the arc is:

$$C = \frac{1}{|1+h_i R_{56}|} \approx \frac{1}{|1+\frac{\sigma_{\delta,i}}{\sigma_{z,i}} R_{56}|} \quad (1)$$

where  $h_i$  is the linear energy correlation with particle's longitudinal coordinate internal to the bunch, normalized to the beam mean energy (linear energy chirp),  $\sigma_{\delta,i}$  and  $\sigma_{z,i}$  are the rms relative energy spread and bunch length,

\* Work supported by Elettra Sincrotrone Trieste and ASML Netherlands B.V. Technology

<sup>†</sup> simone.dimitri@elettra.eu

respectively, all variables intended at the arc entrance;  $R_{56}$  is the linear transport matrix term proportional to the first order momentum compaction of the arc. The approximation in the r.h.s. of Eq.1 is valid as long as the total beam energy spread is dominated by the linear correlation term. Since the maximum FEL peak power is achieved for  $\sigma_{\delta,i} < 0.1\%$ , and given the initial 2 ps bunch length, a relatively large  $R_{56}$  is required in order to obtain a large compression factor, targeting the final peak current of 1 kA at the bunch charge of 100 pC. A large value for  $R_{56}$  implies a large energy dispersion function at the dipole magnets, and, in turn, a large CSR-induced projected emittance growth due to radiation emission and absorption in a dispersive region. Optics strategies to counteract such CSR effect are described in the following.

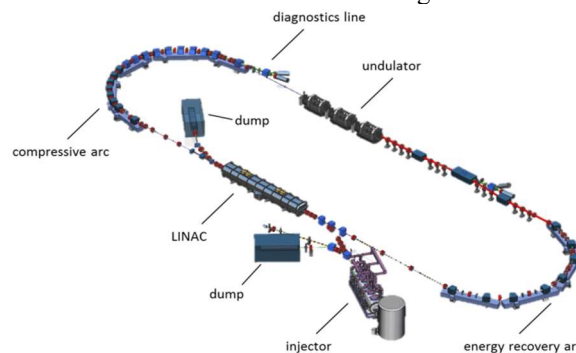


Figure 1: Conceptual scheme of an ERL-FEL; beam moves clock-wise. The scheme is not to scale, and a portion of the straight lines is omitted in order to make the arc lattice more evident. Copyright of APS.

Table 1: ERL-FEL Parameters

Parameter	Value	Unit
Bunch Charge	100	pC
Initial Bunch Duration	2.0	ps
Initial Proj. Norm. Emittance	0.5, 0.5	$\mu\text{m}$
Final Energy	1	GeV
Final Peak Current	1	kA
Final Relative Energy Spread	0.1	%
FEL Wavelength	13.5	nm
FEL Peak Power	1	GW
Arc Compression Factor	56	
Arc $R_{56}$	0.5	m
Proj. Norm. Emittance Growth	$< 0.2$	$\mu\text{m}$

# LCLS-II BEAM CONTAINMENT SYSTEM FOR RADIATION SAFETY\*

C. Clarke<sup>†</sup>, J. Bauer, M. Boyes, Y. Feng, A.S. Fisher, R. Kadyrov, J. Liu, E. Rodriguez, M. Rowen, M. Santana-Leitner, F. Tao, J. Welch, S. Xiao, SLAC National Accelerator Lab, Menlo Park, USA  
T. Allison, Trentronix, LLC, Hampton, USA  
J. Musson, Jefferson Lab, Newport News, USA

## Abstract

LCLS-II is a new xFEL facility under construction at SLAC National Accelerator Laboratory with a superconducting electron linac designed to operate up to 1.2 MW of beam power. This generates more serious beam hazards than the typical sub-kW linac operation of the existing xFEL facility, Linac Coherent Light Source (LCLS). SLAC uses a set of safety controls termed the Beam Containment System (BCS) to limit beam power and losses to prevent excessive radiation in occupied areas. The high beam power hazards of LCLS-II necessitate the development of new BCS devices and a larger scale deployment than previously done at LCLS. We present the new radiation hazards introduced by LCLS-II and the design development for the BCS.

## INTRODUCTION TO LCLS-II

With the LCLS-II upgrade, the complexity and seriousness of potential beam generated hazards at the SLAC FEL facility expands greatly.

LCLS-II adds a second x-ray laser to the already established LCLS x-ray laser, which started operation in 2009 (Fig. 1). LCLS was the first hard x-ray laser and is used by hundreds of scientists each year to deliver 0.3–13 keV x-rays at 120 Hz for imaging at the atomic level and visualisation of femtosecond-scale processes. LCLS-II will operate in parallel with LCLS, introducing new FEL capabilities to operate at up to 1 MHz with x-rays from 250 eV to 25 keV, utilizing Superconducting Radio Frequency (SRF) cavities at 1.3 GHz.

Each accelerator occupies one third of SLAC's existing linear accelerator tunnel. The electron beams traverse nearly 3750 meters of accelerator housing, cover an energy range of up to about 15 GeV for the LCLS (copper cavities) linac beams and above 4.0 GeV for LCLS-II SRF beams, and beam power of up to 250 kW for SRF beams. The SRF beams can simultaneously be sent to two different undulator lines and one additional dump line. The copper linac feeds the hard x-ray undulator only. Laser-like, high power x-ray beams are generated in the undulator lines by the electron beams and traverse another 300 meters to experiment "hutches". There are very many more complex configurations possible and expected in SLAC's future.

The new SRF linac runs CW, and the cryomodule cavities and the RF gun itself can generate beam hazards through field emission that can be captured and accelerated to high

energies. Essentially there are six potential sources for beam related hazards after the LCLS-II upgrade that may be hard to distinguish from each other: Superconducting linac photo-current beam, field emission current generated by the RF Gun for the SRF linac, field emission current generated by superconducting cavities, secondary beam from SRF linac (FEL x-ray beam), copper linac photo-current beam, and secondary beam from copper linac (FEL x-ray beam).

## HISTORY AND DEVELOPMENT OF BCS

A Beam Containment System (BCS), as defined at SLAC, is a set of mechanical, electronic, and electrical devices that limit beam power and beam losses to prevent excessive radiation in occupied areas.

SLAC's original BCS was for the 2-mile long (up to 50 GeV) SLAC accelerator, which could generate nearly 1 MW average beam power and operated up to 8 beamlines. A significant event occurred where 30 W positron beam struck shielding resulting in 360 R/h dose rates outside the 1.8 m concrete shielding [1]. This illustrates the importance of containing the beam before it can hit shielding.

At SLAC, beam is contained with stoppers and protection collimators. A series of tests using 18 GeV electron beam at average powers ranging from 165 kW to 880 kW demonstrated the highly destructive capability of such beams; the rapid burn-through of materials used in the construction of stoppers and collimators (typically seconds if not faster) clearly demonstrated the need for "an extensive electronic system to prevent damage to mechanical devices and to detect onset of destruction" in addition to power monitors, errant beam monitors and burn-through monitors.

The conclusion to these studies was to define the requirements for BCS. The SLAC BCS control system consists of robust, overlapping and type-redundant fault detection devices and beam shut-off systems that provide three functions:

1. To monitor and limit the beam power in a beam line to the allowed value within the capability of the dumps and shielding
2. To limit the losses along a beam line that is operating to its allowed power
3. To protect beam containment devices from damage by sensing when a beam hits it with enough power to damage it

In response to excessive beam power, losses or the risk of damage to beam containment devices, the BCS shuts off the beam using redundant and diverse technologies.

\* Work supported by the U.S. Department of Energy under contract number DE-AC02-76SF00515 and DE-AC05-06OR23177.

<sup>†</sup> cclarke@slac.stanford.edu

# CONSTRUCTION AND OPTIMIZATION OF CRYOGENIC UNDULATORS AT SOLEIL

M. Valléau\*, A. Ghaith, F. Briquez, F. Marteau, P. Berteaud, C. Kitegi, J. Idam, O. Marcouillé, A. Mary, M. Tilmont, J. DaSilva Castro, F. Lepage, K. Tavakoli, J.-M. Dubuisson, N. Béchu, C. Herbeaux, M. Louvet, P. Rommeluère, M. Sebdaoui, A. Lestrade, A. Somogyi, T. Weitkamp, P. Brunelle, L. Nadolski, A. Nadji, M.-E. Couprie, Synchrotron SOLEIL, GIF-sur-YVETTE, France

## Abstract

With permanent magnet undulators operating at cryogenic temperature, the magnetic field and coercivity are enhanced, enabling shorter periods with higher magnetic field. The first full scale (2 m long, 18 mm period) hybrid cryogenic undulator [1] using PrFeB [2] magnets operating at 77 K was installed at SOLEIL in 2011. Photon spectra measurements, in good agreement with the expectations from magnetic measurements, were used for precise alignment and taper optimization. The second and third 18 mm PrFeB cryogenic undulators, modified to a half-pole/magnet/half-pole structure, were optimized without any magnet or pole shimming after assembly, but mechanical sortings and some geometrical corrections had been done before assembly. A systematic error on individual magnets on the third U18 was also compensated. In-situ measurement benches, including a Hall probe and a stretched wire to optimize the undulator field at room and cryogenic temperature are presented. An upgrade of these in-situ benches will be detailed with the fabrication of a 15 mm period and 3 m long PrFeB cryogenic undulator at SOLEIL.

## INTRODUCTION

In-Vacuum Undulators (IVU) generate high magnetic field by placing directly the magnets inside the vacuum chamber. Cryogenic Permanent Magnet Undulators (CPMUs) have been developed to reach intense brightness at higher energies as cooling down  $RE_2Fe_{14}B$  enables to increase the remanent field and coercivity. The first prototype of 0.6 m length with a period of 14 mm, using high remanence  $Nd_2Fe_{14}B$  grade cooled down to 140 K has been developed at SPring-8 [3]. After this first prototype, a 8 x 14.5 mm periods CPMU prototype has been built at Brookhaven National Laboratory (BNL) using  $Nd_2Fe_{14}B$  grade reaching a magnetic gap of 5 mm [4–6]. Helmholtz-Zentrum Berlin (HZB) with the collaboration of UCLA, built two CPMU prototypes (20 x 9 mm period and magnetic gap of 2.5 mm), using  $Pr_2Fe_{14}B$  magnets cooled down to 20-30 K [7]. At SOLEIL, three hybrid prototypes CPMU have been built and characterized: a 4 periods 18 mm length with  $Nd_2Fe_{14}B$  magnets (BH50 Hitachi-Neomax) [8], a 4 x 18 mm period with  $Pr_2Fe_{14}B$  (CR53 Hitachi-Neomax) [9], and a 4 x 15 mm period with  $Pr_2Fe_{14}B$ . The first full-scale cryogenic undulator had been developed at ESRF [10] with a period length of 18 mm

using a relatively low remanence  $Nd_2Fe_{14}B$  magnet grade ( $B_r=1.16$  T) cooled down to around 150 K, reaching a gap of 6 mm. Then full scale undulators using  $Nd_2Fe_{14}B$  based magnets were built for Diamond [11] or at SLS [12]. This article details the design, construction and operation with cryogenic undulators of SOLEIL. U18 n<sup>o</sup>1 was the first full-scale Praseodymium based magnet undulator installed on a storage ring [2]. The second U18 is in use for COXINEL experiment [13, 14] since 2015 and the third one has been installed in the storage ring since Dec. 2017. A 15 mm period and 3 m long cryogenic undulator (U15) operating at 3 mm gap is also under construction.

## MAGNETIC DESIGN

Detailed characterization of  $Re_2Fe_{14}B$  permanent magnets have been carried out at SOLEIL [8]. Figures 1 and 2 show the dependence of the remanence and coercivity as a function of the temperature for  $Nd_2Fe_{14}B$  and  $Pr_2Fe_{14}B$  magnets. When Nd is used, the remanence temperature dependence exhibits a maximum at a temperature between 150 and 100 K, according to the employed grade. It results from the spin transition reorientation (SRT) [15] occurring from this type of magnet. Thus, it requires that Nb based cryogenic undulator to be cooled down to the liquid nitrogen temperature and heated back to the working temperature to 140 K, whereas  $Pr_2Fe_{14}B$  based undulators can be directly cooled and operated at 77 K because of the absence of the SRT. Even larger field can be achieved with  $Pr_2Fe_{14}B$  magnets by cooling even at lower temperatures than the one of the liquid nitrogen. The cryogenics becomes slightly more complex.

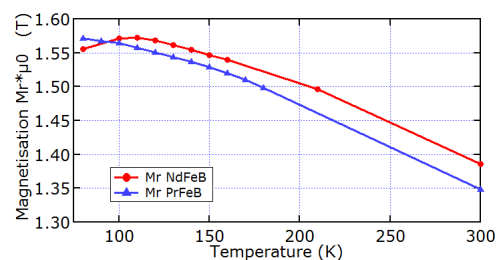


Figure 1:  $Nd_2Fe_{14}B$  (red) and  $Pr_2Fe_{14}B$  (blue) remanent field dependence with the temperature.

\* mathieu.valleau@synchrotron-soleil.fr

## SUMMARY OF WORKING GROUP A (WG-A): LINAC-BASED LIGHT SOURCES

Winfried Decking, DESY, Hamburg, Germany  
Luca Giannessi, Elettra-Sincrotrone, Trieste, and ENEA C.R. Frascati, Italy  
Heung-Sik Kang, Pohang Accelerator Laboratory, Pohang, Korea  
Tor Raubenheimer<sup>†</sup>, SLAC, Menlo Park, CA, USA

### INTRODUCTION

The WG-A program was broken into 6 sessions with 21 invited and contributed talks. A discussion was scheduled at the end of each pair of sessions and a set of questions had been developed to help focus the discussions in the working group. The sessions are listed below along with highlights from the discussions in each section.

### MORE ON NEW FACILITIES

#### *Presentations*

1. **Dong Wang (SINAP)** : *The Shanghai Hard X-ray Free Electron Laser Project*
2. **Tor Raubenheimer (SLAC)** : *Progress on the LCLS-II and the High Energy Upgrade of LCLS-II*
3. **Chang-Ki Min (PAL)**: *PAL-XFEL and its time-resolved experiment with sub-20-fs timing jitter*

There was no focused discussion on the new facilities although the tour on Friday took us through the Shanghai Synchrotron Radiation Facility (SSRF) and the Soft X-ray FEL (SXFEL) at SINAP.

### MACHINE OPTIMIZATION

#### *Presentations*

1. **Daniel Ratner (SLAC)**: *Report on an ICFA BD mini-workshop on “Machine learning for particle accelerators”*
2. **Lars Fröhlich (DESY)**: *Automated Optimization of Machine Parameters at the European XFEL*
3. **Zeng Li (SINAP)**: *The Feasibility of Neuron Network-Based Beam-Based Alignment*
4. **Haeryong Yang (PAL)**: *FEL optimization through BBA with undulator spectrum analysis and undulator optics matching*

#### *Focus Questions and Discussion:*

1. What are the optimization strategies used in tuning a single pass, linac-based FEL for user operation?
2. Will artificial intelligence play a role in tuning and optimizing FEL sources?
3. What are the main differences between the optimization strategies in 3rd and 4th generation light sources?

\* This work supported in part by DOE Contract No. DE-AC02-76SF00515.

<sup>†</sup> torr@stanford.edu

**Machine preparation is time consuming, automatic optimization reduces the preparation times and frees operators from repetitive annoying procedures. It reduces the possibility of errors and may help in retrieving conditions that are operator independent. Furthermore, the **tighter tolerances in 4<sup>th</sup> generation facilities may prevent them from relying simply on “design models”** because the real system is only partially known and diagnostics do not provide a complete picture. In this case, **automatic optimization becomes essential** to achieve the maximum performance in a reasonable time.**

**Artificial intelligence techniques are starting to be used to create more accurate “models.”** Some examples of applications include reconstruction of machine conditions by analysing large amount of stored data and running virtual machines to train optimizers. **In the next generation photon sources, automatic optimizations and machine learning with AI is also playing a role in the design phase** (see CompactLight design study, A. Latina in WG-C). **Interesting cases of non-trivial unexpected behaviors are being “discovered” by optimizers** with advanced algorithms, as the taper optimization (D. Ratner report WG-A). This is **very promising** for the future.

### SCHMES FOR PRODUCTION OF ULTRASHORT PULSES IN EUV AND X- RAY FELS

#### *Presentations*

1. **James Mac Arthur (SLAC) on behalf of A. Marinelli, J. Duris, & XLEAP team**: *X-ray Laser-Enhanced Attosecond Pulses*
2. **Xi Yang (BNL) (presented by Luca Giannessi)**: *Generation of atto-second pulses in FELs: Ultrashort pulse generation and superradiance*
3. **Neil Thompson (STFC/DL/ASTeC)**: *Free-Electron Laser R&D in the UK - steps towards a national XFEL facility*

#### *Focus Questions and Discussion:*

1. What are the main challenges and desiderata in the generation of ultrashort pulses in FELs?
2. What are the strategies for temporal synchronization of ultrashort (sub-fs) FEL pulses and of the light properties?

## WG-B: RING BASED LIGHT SOURCES - SUMMARY

Y. Li, BNL, Long Island, New York, USA  
Q. Qin, IHEP, Beijing, China  
R.P. Walker, DLS, Daresbury, UK

### WORKING GROUP TOPICS

In the six Working Group B sessions there were 21 oral presentations which included:

i/ overviews of many of the current ring based light source projects that are underway or being studied around the world: APS-U, BESSY-VSR, ESRF-EBS, Elettra 2.0, HALS, HEPS, KEK-LS, PETRA IV, SOLEIL upgrade, SPS-II,

ii/ various reviews of ‘hot topics’ such as injection schemes (Z. Duan), short pulse schemes (A. Jankowiak), round beam challenges (P. Kuske, plenary talk) and collective effects (R. Nagaoka),

iii/ more specific talks on topics such as ion effects, impedances, transient beam loading and less conventional ring-based light source schemes.

WG-B was asked to consider the following questions:

- Are there new ideas for storage ring lattices that could go beyond currently-envisioned MBA lattices?
- Should we be making more use of permanent- or superconducting-magnet technologies?
- Should new facilities plan for a full-energy linac injector to allow pushing the ring as far as possible?
- How can we make short lifetimes workable, so we can continue pushing the emittance down?
- What theory and code developments do we need to ensure that next-generation rings work as planned?
- What experiments can be performed on existing rings to remove uncertainties for next-generation rings?
- Besides rings optimized for ultra-high-brightness, what other types of rings should we be designing?
- What's needed to make first-principles impedance models more accurate in predicting instabilities?
- What commissioning strategies are best for next-generation rings?
- How do storage ring design and beamline design interact; e.g., round vs flat beams, tailoring of beta functions vs lowest emittance?
- Can ultra-bright rings also provide short pulses?
- Is low emittance more demanding of insertion device quality, e.g., phase errors?
- Are there new beam stability challenges and what are the best ways to address these?

Although neither the presentations nor the discussions addressed these questions directly, in the following we will nevertheless attempt to make some relevant comments based on the content of the presentations at FLS2018.

### RESPONSES TO QUESTIONS

*Are there new ideas for storage ring lattices that could go beyond currently-envisioned MBA lattices?*

The hybrid MBA lattice of ESRF-EBS has been adopted for APS-U and HEPS and is the current baseline lattice for PETRA IV and the SOLEIL upgrade. Anti-bends are incorporated in APS-U and in one option for HEPS (with anti-bends and superbends).

Z. Bai presented various MBA lattices with sextupoles distributed throughout the cell for HALS; these have additional symmetry planes and odd- $\pi$  phase advance in both planes across the mid-plane. 6BA and 8BA lattices were presented with emittances of 26-36 pm at 2.4 GeV with DA of  $\pm 1.5$ -2 mm and large MA. A further MBA lattice type with two pairs of interleaved dispersion bumps with  $-I$  transformation between each was presented; a 7BA version of this produces 32 pm natural emittance with DA of  $\pm 3$  mm and large MA. Adding longitudinal gradient bends, anti-bends, and 2T superbends produces a lattice with 23 pm emittance and similar DA/MA.

I. Agapov presented an alternative lattice for PETRA IV with “double  $-I$  optics”: in the first part of the arc there is  $\pi$  phase advance between points of maximum dispersion and  $\beta_x$ , and in the second part there is  $\pi$  phase advance between points of maximum  $\beta_y$ . This was said to require further development, but looks promising.

In other cases the desire for the lowest possible emittance has been compromised for the advantage of gaining additional straight section space in the middle of the arc where insertion devices or other components can be located. What generically might be called “split-MBA” lattices are being considered for Elettra 2.0 (6BA), SPS-II (6BA) and KEK-LS (8BA).

*Should we be making more use of permanent- or superconducting-magnet technologies?*

We believe that permanent magnet technology in particular has many benefits for future light sources. In a first development of this kind, ESRF-EBS will use permanent magnet longitudinal gradient dipoles. In WG-D, A. Vorozhtsov presented a very interesting design of a high gradient (234 T/m) permanent magnet quadrupole with bore radius of 5.5 mm for possible application in a future upgrade of MAX-IV. The design presented has a tuning range of  $\pm 5\%$  which might limit the flexibility of the lattice.